
RANDOM ABSTRACT CELL COMPLEXES

A PREPRINT

Josef Hoppe*

Department of Computer Science
RWTH Aachen University
Aachen, Germany
hoppe@cs.rwth-aachen.de

Michael T. Schaub

Department of Computer Science
RWTH Aachen University
Aachen, Germany
schaub@cs.rwth-aachen.de

ABSTRACT

We define a random model for (abstract) cell complexes (CCs), similar to the well-known Erdős–Rényi model for graphs and its extensions for simplicial complexes. To build a random cell complex, we first draw from an Erdős–Rényi graph, and consecutively augment the graph with cells for each dimension with a specified probability. As the number of possible cells increases combinatorially — e.g., 2-cells can be represented as cycles, or permutations — we derive an approximate sampling algorithm for this model limited to two-dimensional abstract cell complexes. As a basis for this algorithm, we first introduce a spanning-tree-based method that samples simple cycles and allows the efficient approximation of various properties, most notably the probability of occurrence of a given cycle. This approximation is of independent interest as it enables the approximation of a wide variety of cycle-related graph statistics using importance sampling. We use this to approximate the number of cycles of a given length on a graph, allowing us to calculate the sampling probability to arrive at a desired expected number of sampled 2-cells. The probability approximation also trivially leads to a sampling algorithm for 2-cells with a desired sampling probability. We provide some initial analysis into the properties of random CCs drawn from this model. We further showcase practical applications for our random CCs as null models, and in the context of (random) liftings of graphs to cell complexes. The cycle sampling, cycle count estimation, and combined cell sampling algorithms are available in the package `py-raccoon` on the Python Packaging Index.

Keywords Random Models · Null Models · Random Abstract Cell Complexes · Simple Cycles · Higher-Order Networks

1 Introduction

Since the seminal work of Erdős–Rényi [1], random models of relational data described by graphs have been a mainstay topic of interest within probability theory, statistics, data science and machine learning. The interest in such random graphs can be motivated from at least three perspectives. First, they are vital as generative models for complex networks in various disciplines, including social sciences, physics, and biology [2, 3], as they enable the theoretical and empirical study of how certain (random) connection mechanisms can influence the make-up of a network. Second, random models can serve as null models to evaluate whether some observed network statistics may be deemed significant. Third, random models can generate synthetic input data for training machine learning models, or for controlled experiments and benchmarking of network analysis algorithms.

Starting from the Erdős–Rényi (ER) model [1] and its variation by Gilbert [4], a vast array of models for random graphs has been developed, such as the Stochastic Block Model [5], the Configuration Model [6], etc. (see Appendix A for more related literature). Many of these models allow for the direct or indirect specification of certain network statistics — e.g., density, triangle counts, degree distribution — to be preserved (either exactly or in expectation) in samples drawn from the model.

*<https://hoppe.io>

Evaluation Code and PyPI Package available at github.com/josefhoppe/random-abstract-cell-complexes.

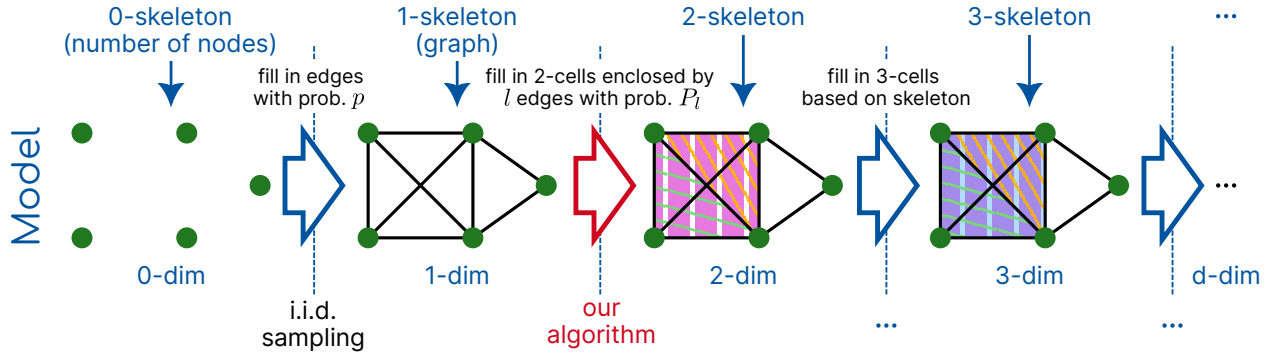


Figure 1: Overview of the random abstract cell complex model. The model is defined through iterative liftings from d to $d + 1$ -dimensional cell complexes. This makes it possible to fix a skeleton of the complex and only apply the random lifting for subsequent dimensions. In this paper, we focus on the lifting from one- to two-dimensional abstract cell complexes. For this, we present a novel, efficient approximate sampling algorithm (see Figure 4).

Recently, there has been a trend in studying higher-order network models such as hypergraphs and simplicial and cellular complexes [7, 8, 9]. These richer models for relational data have gained interest as they enable the study of complex network structures with interactions beyond pairwise relationships, which have been deemed to be essential to model certain systems. In contrast to random graph models, the landscape of models for these higher-order networks is however far less developed (see appendix for related work). In particular, even though (abstract) cell complexes feature prominently in topological data analysis [10], and in the emerging areas of topological signal processing [11, 12] and topological deep learning [13], currently, the only practically usable models for random cell complexes are ill-defined ad hoc models [14]. Appendix A provides a more in-depth overview of related work.

Contributions. We define a general model for random abstract cell complexes. Our model for random abstract cell complexes that generalizes the Linial-Meshulam model [15, 16] for SCs, but may also be used to lift a graph to a 2-dimensional cell complex. Sampling from this model is non-trivial due to combinatorial complexity. Thus, we provide an algorithm that lifts graphs to 2-dimensional cell complexes by randomly adding cells. In practice, it is usually desirable to sample 2-dimensional cell complexes with a certain *number* of 2-cells rather than a fixed probability. We present two related algorithms to achieve this: First, an algorithm that **approximates the total number of cycles** of each length, which is both of independent interest and makes it possible to set a sampling probability for cycles. Second, an (approximate) algorithm that **samples 2-cells (cycles) with a given probability**. We provide an open source implementation of both algorithms in python. Finally, we demonstrate the utility of our random cell complex model: we briefly analyze the orientability and homologies of sampled complexes; use it as a null model to create an evaluation baseline; and demonstrate the use of random liftings to gain insight to neural networks defined on cell complexes [17].

Outline. In the remainder of this paper, we first introduce relevant concepts and notation in Section 2 before presenting our random cell complex model in Section 3. We then introduce our spanning-tree-based method to explore the set of cycles on a graph in Section 4. This forms the basis for our approximate cycle counting in Section 5 and our cell sampling algorithm in Section 6. We analyze our algorithm both theoretically in Section 7 and empirically in Section 8. Finally, we investigate properties of random cell complexes in Section 9 and provide case studies of applications of random CCs in Section 10.

2 Background and Notation

Graphs and simple cycles. We consider undirected graphs $G = (V, E)$ with $n := |V|$ nodes and $m := |E|$ edges. An Erdős-Rényi random graph $G(n, p)$ has n nodes and for any node pair $u, v \in V$, the edge (u, v) exists independently with probability p . A cycle c is a closed simple path on G ; its length $|c|$ equals the number of nodes (or edges) in c . We denote the set of all cycles in G by C . We use C_l to denote the set of all cycles $c \in C$ with length $|c| = l$ and $N_l = |C_l|$ to denote the number of cycles on a graph. If node u or edge (u, v) is part of the cycle c , we write $u \in c$ or $(u, v) \in c$, respectively. We assume, without limiting generality¹, that all graphs are connected.

¹On a graph with multiple connected components, we can consider each component separately.

Algorithm 1 RCC iterative lifting algorithm.

Input: CC C , d_{\max} , $P^{(d)}$ for $\dim C < d < d_{\max}$
for $d \leftarrow (\dim C + 1)..d_{\max}$ **do**
 for l s.t. $P_l^{(d)} > 0$ **do**
 $X \leftarrow \forall$ possible cells c with boundary size l : select independently with probability $P_l^{(d)}$
 $C \leftarrow C \cup X$
 end for
end for
return C

Cycle bases and spanning trees. The cycle space of a graph is the set of its subgraphs in which every node has even degree. With addition defined as the symmetric difference and scalar multiplication with \mathbb{F}_2 , the cycle space is a vector space. A *cycle basis* is a set of *simple* cycles that is a basis of the cycle space. Any spanning tree T on a graph G induces a cycle basis [18]: Each edge (u, v) that is not in T closes the path from u to v on T , creating a simple cycle; the set of all induced cycles C_T is a cycle basis on G .

Uniform spanning trees and the Laplacian Random Walk. A uniform spanning tree is a spanning tree picked uniformly at random from all spanning trees on a given graph. Uniform spanning trees can be efficiently obtained by Wilson’s algorithm [19]. The probability of a certain path being included in a uniform spanning tree can be calculated via a particular absorbing random walk termed the Laplacian random walk [20].

Abstract Cell Complexes. In general, abstract cell complexes are a generalization of graphs, adding higher-dimensional structure (cells). k -cells are simple k -dimensional volumes, for example 2-cells are polygons, 3-cells are polyhedra, etc. Cells are attached to their boundary, a set of $k - 1$ -dimensional cells forming a simple cycle, a sphere, etc. Simplicial complexes are a special case of cell complexes, limiting cells to be simplices, i.e., all polygons are triangles, all polyhedra are tetrahedra, etc.

From here on, we will use the term *cell complex* to refer to *abstract* cell complexes. While the model introduced in this paper (cf. Figure 1) considers cell complexes of arbitrary dimension, our sampling algorithm is limited to two-dimensional cell complexes. For the purpose of this paper, we may simply think of a 2-dimensional cell complex as a graph with additional 2-cells (polygons) that are attached to simple cycles on the graph. For a more formal and complete introduction, we refer the reader to [21]

3 A Model for Random Abstract Cell Complexes

Random abstract cell complexes can be sampled through a series of iterative liftings that each lift a d -dimensional complex to a $(d + 1)$ -dimensional complex, as illustrated in Figure 1. The first lifting, from a 0-dimensional cell complex (set) to a 1-dimensional cell complex (graph), adds 1-cells (edges) with a fixed probability and is equivalent to the Erdős–Rényi model. For two- and higher-dimensional cells, the number of possible cells depends on the size of the boundary (e.g. edges for 2-cells). To avoid only sampling cells with, e.g., very large boundaries, for every dimension d and possible boundary size l , we define the inclusion probability $P_l^{(d)}$. We define our random cell complex model $\text{RCC}(n, P^{(1)}, \dots, P^{(d_{\max})})$, where the vector $P^{(i)} = (P_l^{(i)})$ collects the inclusion probabilities of i -cells with boundary size l (cf. Algorithm 1). Each possible cell is added independently according to the inclusion probability (i.e., depending on the boundary size). For dimension $d = 2$ and above, the cells that can be added depend on the sampled cells from dimension $d - 1$. This iterative lifting-based model also allows us to augment any given CC with random higher-dimensional cells of specified dimensions.

Relationship to the Erdős–Rényi model. For 1-cells (edges), the only possible boundary size is 2. Therefore, the model $\text{RCC}(n, P^{(1)})$ is equal to $\text{ER}(n, P_2^{(1)})$.

Relationship to the Linial-Meshulam model. The RCC model can be seen as a generalization of the LM model. Specifically, to recover the LM model, we set $P_{d+1}^{(d)} = 1$ for all dimensions d except d_{\max} , resulting in a full simplicial complex. Then, by setting $P_{d_{\max}+1}^{(d_{\max})} = p$ and all other inclusion probabilities to 0, we obtain the LM model.

Sampling 2-cells on a graph. As a step towards a sampling algorithm for the full model described above, we consider algorithms for the lifting from one-dimensional CCs (graphs) to two-dimensional CCs. As there is no risk of confusion in this context, we simply use P_l to refer to $P_l^{(2)}$ in the following.

3.1 Heterogeneity for static target probability P_l

Different realizations of Erdős–Rényi graphs with the same parameters have differ a lot in the number of cycles for each length (see Figure 12). Thus, if we sample 2-cells with a fixed probability P_l , there will be a similar variance in the number of sampled 2-cells. This behavior is undesirable in many applications as it leads to variations in the dimension of the cycle space, connectivity, and eigenvalues of the Hodge Laplacian. If required, this behavior can be changed by adjusting $P^{(2)}$ based on the realization of the 1-skeleto This poses a new challenge as number of simple cycles is not easy to obtain. Thus, we also propose an algorithm to approximate the number of simple cycles in Section 3.1

3.2 Practical Considerations for Sampling 2-Cells

Before introducing our sampling algorithm, we discuss adoptions of widely-used sampling procedures, showing that they are not practical for this problem.

Rejection sampling for liftings of (nearly) complete graphs. Rejection sampling is a general approach that can be used here by sampling random permutations of length l and rejecting those that do not form valid cycles in G . The rejection rate depends on the underlying graph. If we assume the graph to be sampled from ER, then one of p^{-l} permutations is a valid boundary of a 2-cell of length l , in expectation. Therefore, rejection sampling is well-suited only for sampling of short cells or on (almost) complete graphs, but too computationally complex in other cases.

Markov Chain Monte Carlo. MCMC algorithms sample from a probability distribution via random walks on all possible values, connected by a move set. A simple move set on simple cycles would be the symmetric difference with any set of simple cycles. However, this space may not be connected, e.g., on the graph of two triangles connected by an edge $(\triangleleft\triangleright)$. Therefore, an MCMC algorithm would require a more complex move set, i.e., there is no trivial Markov chain Monte Carlo algorithm for sampling simple cycles.

4 Taming the Cycle Space with Spanning Trees

In the previous section, we saw that the set of simple cycles on arbitrary graphs is complex and difficult to analyze. Therefore, in this section, we introduce a general method to explore the cycle space that is based on spanning trees. This provides a biased sample. By approximating the bias, we can then correct for it. In the following sections, we will use this method to both approximate the number of cycles and implement the sampling algorithm for 2-cells.

Spanning trees are a dual concept to cycles: A spanning tree is specifically a maximal subgraph that does not contain a cycle. Thus, by adding any additional edge, we can find a cycle. In this way, a spanning tree T induces a set of cycles C_T . Spanning trees can be sampled uniformly from the set of all trees \mathbb{T} efficiently using Wilson’s algorithm [19]. Furthermore, some calculations, e.g. calculating the length of an induced cycle, can be performed efficiently on the spanning tree.

In this section, we will combine these properties to uniformly sample a spanning tree $T \in \mathbb{T}$ and, for each induced cycle $c \in C_T$, approximate its probability $\rho_c = |\{T : c \in C_T\}| / |\mathbb{T}|$ of being induced by a uniformly sampled spanning tree. It returns the spanning tree T and a set of tuples $(u, v, \text{lca}(u, v), \tilde{\rho}_c)$, where (u, v) is the edge added, $\text{lca}(u, v)$ is the lowest common ancestor of u and v in T , and $\tilde{\rho}_c$ is the approximated occurrence probability.

Instead of iterating the induced cycles, we determine the lowest common ancestor of all pairs of nodes that form a non-tree edge. From the lowest common ancestor, we can calculate some properties of the cycle in constant time. For example, the length of the cycle induced by the edge (u, v) can be calculated from the depth of both nodes and the lowest common ancestor in T (with an arbitrary root). The approximation of the occurrence probability $\tilde{\rho}_c$ is also designed to be calculated in a similar fashion. Section 7.1 analyzes the computational complexity of the full approach. The reader may choose to take this method as a black box and move on to the next sections as the details are not required to understand the algorithms that are built on top.

Wilson’s algorithm [19] generates uniform spanning trees by choosing an arbitrary root r and, for every other vertex v , takes a loop-erased random walk until reaching a node in the tree, adding all visited nodes. As the name suggest, a loop-erased random walk from u to v can be obtained by performing a standard random walk from u to v and removing

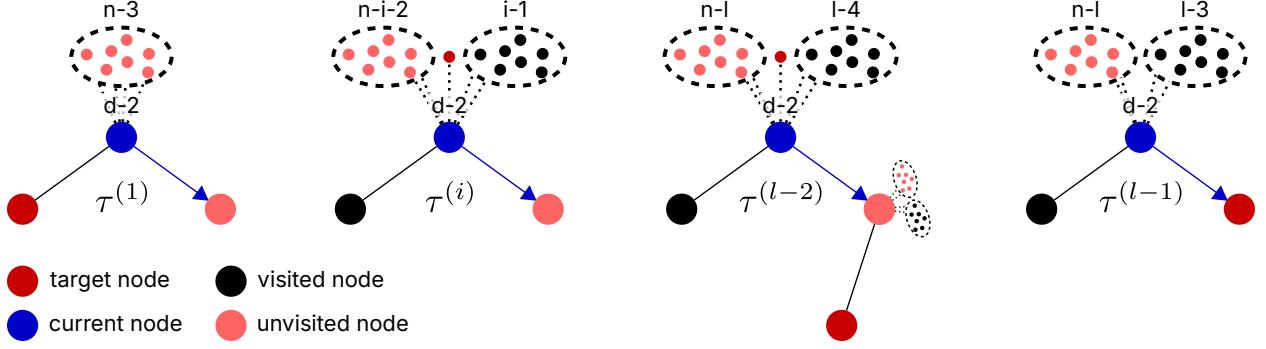


Figure 2: Approximation of the transition probabilities $\tau_c^{(i)}$ of the Laplacian Random Walk. The node to the left is always the previous node in the walk (or, for the first step, the target node). In the general case $\tau_c^{(i)}$, we know that one neighbor is visited and one neighbor is unvisited. All other neighbors are assumed to be equally likely, i.e., the $d - 2$ remaining neighbors' probability is averaged over the visited, unvisited, and target nodes. In the first step, we know that the target node is a neighbor of the current node, reducing the probability of taking the exact path. In the penultimate step $\tau_c^{(l-2)}$, the next node on the path has a higher probability of being chosen because it is certainly adjacent to the target node. In the final step $\tau_c^{(l-1)}$, the next node is the target node and thus has a higher probability of being chosen.

all loops in the walk. The probability of a path from u to v being part of a uniform spanning tree is the same probability as the loop-erased random walk between the two ends choosing this path [19].

The Laplacian random walk [20] has the same probability distribution as the loop-erased random walk, but instead of choosing the next node uniformly and deleting parts afterwards, in every step, it assigns different probabilities to different neighbours. Intuitively, each node's value corresponds to the probability of a random walk not resulting in a loop. For visited nodes, this probability is 0 as choosing them would immediately result in a loop. For the target node, the probability is 1 as choosing it ends the walk without creating a loop. For all other nodes, this probability is the average of their neighbors as they would be chosen uniformly in the next step.

Formally, let t be the target node and V_i' the set of visited nodes in step i . The transition probability is defined by a probability density vector $f \in C_0$, s.t. $\forall v \notin V_i', v \neq t: (Lf_i)_u = 0, f_t = 1$, and $\forall v \in V_i': f_v = 0$.

Each cycle c is induced by a spanning tree if and only if it includes any path consisting of all but one edge of c . Thus, we need to calculate the probability of multiple Laplacian random walks to arrive at the occurrence probability ρ_c . We denote the transition probability of every step by τ_c^i . In Appendix B, we approximate this probability, incorporating the structural information we have available as shown in Figure 2.

First, we present approximations for f_i . In the general case, we can use $\tilde{f}_i = 1/i+1$. For neighbors of the current node, we use \tilde{f}_i' ; and for the penultimate step, where the next node is a neighbor of both the current and the target node, we use \tilde{f}_i'' .

$$\tilde{f}_i' = \frac{\tilde{d} - 1}{\tilde{d}} \frac{n - 1}{n - 2} \frac{1}{i + 1} \quad (1)$$

$$\tilde{f}_{l-2}'' = \frac{1 + \frac{\tilde{d}-2}{n-3} \frac{n-l}{l-1}}{\tilde{d}} \quad (2)$$

For the transition probabilities, we distinguish five cases. In general, we have probabilities $\tilde{\tau}_c^{(i)}$ and the less accurate but easier to compute version $\tilde{\tilde{\tau}}_c^{(i)}$. Furthermore, we have separate probabilities $\tilde{\tau}_c^{(1)}, \tilde{\tau}_c^{(l-2)}, \tilde{\tau}_c^{(l-1)}$ for the first and last two steps, respectively.

$$\tilde{\tau}_c^{(1)}(n, d, \tilde{d}) = \frac{1}{2 \frac{\tilde{d}}{d-1} \frac{n-2}{n-1} + d - 1} \quad (3)$$

$$\tilde{\tau}_c^{(i)}(n, d, i) = \frac{1}{1 + (d-2) \frac{1}{n-3} (n-i-2 + \tilde{f}_i'^{-1})} \quad (4)$$

$$\tilde{\tau}_c^{(i)}(n, d) = \frac{1}{1 + (d-2) \frac{n-1}{n-3}} \quad (5)$$

$$\tilde{\tau}_c^{(l-2)}(n, d, l) = \frac{\tilde{f}_{l-2}''}{\tilde{f}_{l-2}'' + (d-2) \frac{1}{n-3} ((n-l)\tilde{f}_{l-2} + 1)} \quad (6)$$

$$\tilde{\tau}_c^{(l-1)}(n, d, l) = \frac{1}{1 + (d-2) \frac{n-l}{n-3} \tilde{f}_{l-1}'} \quad (7)$$

Finally, we assemble these into the overall occurrence probability of a cycle:

$$\gamma(n, \tilde{d}, l) = \left(\prod_{i=2}^{l-2} \frac{\tilde{\tau}_c^{(i)}(n, \tilde{d}, i)}{\tilde{\tau}_c^{(i)}(n, \tilde{d})} \right) \frac{\tilde{\tau}_c^{(l-2)}(n, \tilde{d}, l)}{\tilde{\tau}_c^{(i)}(n, \tilde{d})} \frac{\tilde{\tau}_c^{(l-1)}(n, \tilde{d}, l)}{\tilde{\tau}_c^{(i)}(n, \tilde{d})} \quad (8)$$

$$\eta(n, u, v) = \frac{\tilde{\tau}_c^{(1)}(n, d(u)) + \tilde{\tau}_c^{(1)}(n, d(v))}{2 \tilde{\tau}_c^{(i)}(n, d(u)) \tilde{\tau}_c^{(i)}(n, d(v))} \quad (9)$$

$$\varrho(n, u) = \tilde{\tau}_c^{(i)}(n, d(u)) \quad (10)$$

$$\tilde{\rho}_c = \gamma(n, \tilde{d}, l) \left(\sum_{(u,v) \in c} \eta(n, u, v) \right) \prod_{u \in c} \varrho(n, u) \quad (11)$$

5 An Approximate Algorithm for Counting Cycles on a Graph

As explained previously, a good approximation of the number of cycles $N_l = |C_l|$ on a graph is important to properly configure RCC in practice. In this section, we present an approximation for N_l based on the spanning-tree-based cycle sampling from the previous section. We provide three different intuitions for the derivation of the approximation. First, we can think of this as an importance sampling problem. Second, we may think of this as a maximum likelihood estimation over binned probabilities. Finally, we give an counting based on an enumeration of all spanning trees, and derive our approximation as a subsampling of this enumeration.

All three intuitions lead to the same approximation based on the induced sets of cycles C_{T_i} of s spanning trees T_1, \dots, T_s :

$$N_l \approx \frac{1}{s} \sum_{i=1}^s \sum_{c \in C_l \cap C_{T_i}} \frac{1}{\rho_c} \quad (12)$$

By approximating $\rho_c \approx \tilde{\rho}_c$, we can use the efficient cycle sampling algorithm to retrieve an estimation of N_l .

Importance Sampling. Importance sampling is a sampling technique to estimate the expected value of a property $f(x)$ under a probability distribution $p(x)$ on a set X , where $p(x)$ is difficult to sample from. Instead, we sample from a different distribution $q(x)$ and correct for the bias. If $q(x) > 0$ where $p(x) > 0$, instead of estimating $\mathbb{E}_{x \sim p}[f(x)] \approx \frac{1}{s} \sum_{k=1}^s f(x_k)$, $x_k \sim p$, we can estimate $\mathbb{E}_{x \sim p}[f(x)] = \mathbb{E}_{x \sim q}[\frac{p(x)}{q(x)} f(x)] \approx \frac{1}{s} \sum_{k=1}^s \frac{p(\hat{x}_k)}{q(\hat{x}_k)} f(\hat{x}_k)$, $\hat{x}_k \sim q$. For a full introduction, we refer the reader to [22].

We can efficiently sample simple cycles from the distribution q that first uniformly samples a spanning tree T and then uniformly samples a cycle from the induced set of cycles of length $C_T \cap C_l$. Note that, in general, $C_T \cap C_l$ may be empty, although it is very unlikely. For this intuition, we accept that this does not work in practice and assume that

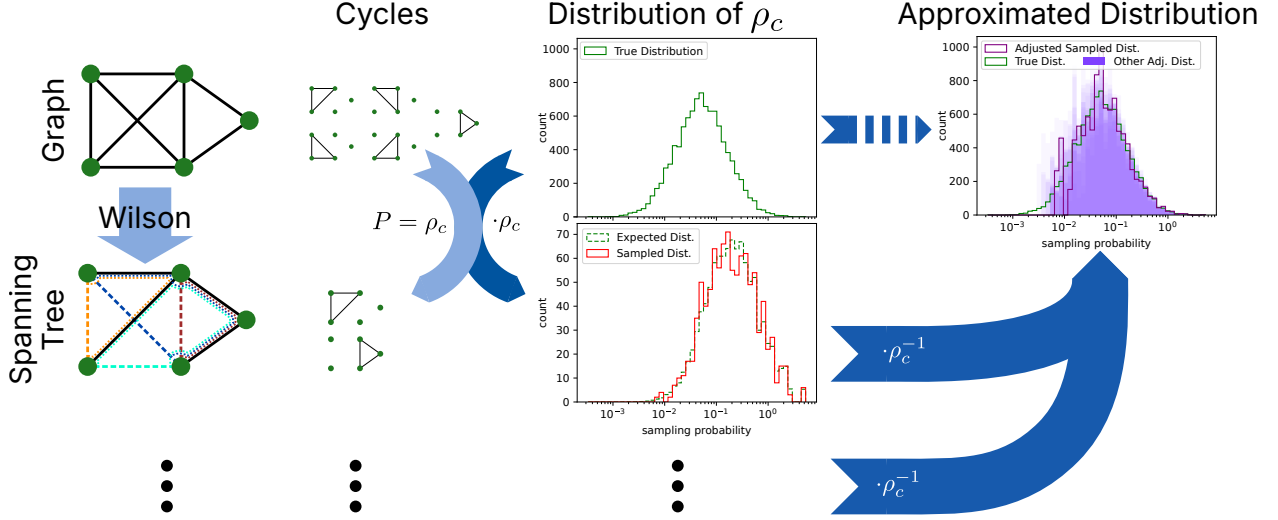


Figure 3: **Estimating a distribution of sampling probabilities from sampled objects and their probabilities.** The top row shows a graph, its cycles, and the distribution of the occurrence probabilities of the cycles. The goal is to approximate the distribution (dotted arrow) efficiently. To do this, we sample multiple uniform spanning trees. Such a spanning tree (bottom row) also effectively samples a set of (induced) cycles. The distribution of these cycles is, in expectation, the correct distribution multiplied with the occurrence probability. By multiplying the sampled distribution with the inverse of the occurrence probability, we get an approximation of the true distribution. The final approximation is the average over all approximations we obtained from different spanning trees.

$C_T \cap C_l \neq \emptyset$, and retrieve $q(c) = \rho_c \cdot |C_T \cap C_l|$. We will resolve this by departing from the intuition of importance sampling. To estimate the number of cycles, we set $p(c) = 1/|C_l|$ as the uniform distribution over all cycles of length l and choose $f(c) = |C_l|$, i.e., we take the expectation over all cycles of the constant that is the cycle count. This gives the following equation:

$$N_l = |C_l| = \sum_{c \in C_l} 1 = \sum_{c \in C_l} \overbrace{|C_l|}^{f(c)} \cdot \overbrace{\frac{1}{|C_l|}}^{p(c)} = \sum_{c \in C_l} f(c) \cdot p(c) \quad (13)$$

$$\approx \frac{1}{s} \sum_{i=1; c_i \sim C_p} f(c_i) = \frac{1}{s} \sum_{i=1; c_i \sim C_q} \frac{p(c_i)}{q(c_i)} \cdot f(c_i) = \frac{1}{s} \sum_{i=1; c_i \sim C_q} \frac{1}{q(c_i)} \frac{1}{|C_l|} \cdot |C_l| = \frac{1}{s} \sum_{i=1; c_i \sim C_q} \frac{1}{q(c_i)} \quad (14)$$

Given a sampled tree T and assuming that $C_T \cap C_l \neq \emptyset$, it is possible to calculate the expectation:

$$\mathbb{E}_{c \sim C_T \cap C_l} \left[\frac{1}{q(c)} \right] = \mathbb{E}_{c \sim C_T \cap C_l} \left[\frac{|C_T \cap C_l|}{\rho_c} \right] = \sum_{c \in C_T \cap C_l} \frac{1}{\rho_c} \quad (15)$$

This equation also gives a result if $C_T \cap C_l = \emptyset$, as the expectation is then 0. In other words, if no cycles of length l are induced by a spanning tree, we estimate that there are no cycles of length l on the graph. The other intuitions will confirm that this is the correct interpretation. We can now substitute the sampling process to obtain q with sampling one uniform spanning tree and then substitute the expectation:

$$N_l \approx \frac{1}{s} \sum_{i=1}^s \sum_{c \in C_l \cap C_{T_i}} \frac{1}{\rho_c} \quad (16)$$

Subset Sampling. Alternatively, we may think of the spanning-tree-based sampling more generally as sampling a subset from the set of all cycles, with different probabilities. Using our sampling process, we may think of the set of all cycles as a set C of pairs (c, ρ_c) where we sample each pair with probability ρ_c . Note that we do not represent c

explicitly in the final equation, but use it only in the derivation. We call the set of sampled cycles C' . Figure 3 shows an example for the general case of sampling this, and how to adjust for probabilities.

We perform the following separately for each cycle length l . We can bin the occurrence probabilities ρ_c into m bins $([b_i, b_{i+1}))_{1 \leq i < m}$ and estimate how many cycles fall into each bin. If there are n_i cycles in the set of all cycles that fit into bin $[b_i, b_{i+1})$, we would sample approximately $b_i \cdot s \cdot n_i$ cycles in the bin (in expectation; possibly sampling a cycle multiple times). In reverse, given n'_i sampled cycles in a bin, we can estimate $n_i \approx n'_i / b_i \cdot s$. The total number of cycles of length l can then be estimated by summing over all bins:

$$N_l = \sum_{i=1}^m n_i \approx \sum_{i=1}^m \frac{n'_i}{b_i \cdot s} = \sum_{i=1}^m \frac{|\{c \in C'_l : b_i \leq \rho_c < b_{i+1}\}|}{b_i \cdot s} \quad (17)$$

Similar to approximating an integral via a lower sum, we can increase accuracy by reducing the size of the bins. If we take the limit of $b_{i+1} - b_i \rightarrow 0$, this results in a single probability (possibly representing multiple cycles that share a probability) for each bin:

$$N_l \approx \sum_{i=1}^m \frac{|\{c \in C'_l : b_i \leq \rho_c < b_{i+1}\}|}{b_i \cdot s} \stackrel{\lim_{b_{i+1} - b_i \rightarrow 0}}{=} \sum_{b_i} \frac{|\{c \in C'_l : \rho_c = b_i\}|}{b_i \cdot s} = \sum_{c \in C_l} \frac{1}{\rho_c \cdot s} = \frac{1}{s} \sum_{i=1}^s \sum_{c \in C_l \cap C_{T_i}} \frac{1}{\rho_c} \quad (18)$$

Subsampling All Spanning Trees. We may also think of this equation as subsampling the enumeration of all spanning trees. Given a graph G , let \mathbb{T} be the set of all spanning trees of G and $\mathbb{T}_c := \{T \in \mathbb{T} : c \in C_T\}$ the set of all spanning trees that induce a given cycle c . Note that the occurrence probability ρ_c of a cycle c can be expressed in terms of the cardinalities of these sets of spanning trees, i.e., $\rho_c = |\mathbb{T}_c|/|\mathbb{T}|$. In the limit, where we iterate over all trees \mathbb{T} and the number of samples $s = |\mathbb{T}|$ is the number of all spanning trees, this exactly counts all cycles:

$$N_l = |C_l| = \sum_{c \in C_l} 1 = \sum_{c \in C_l} \sum_{T \in \mathbb{T}_c} \frac{1}{|\mathbb{T}_c|} = \sum_{T \in \mathbb{T}} \sum_{c \in C_l \cap C_T} \frac{1}{|\mathbb{T}_c|} = \sum_{T \in \mathbb{T}} \sum_{c \in C_l \cap C_T} \frac{1}{\rho_c |\mathbb{T}|} \quad (19)$$

We can approximate \mathbb{T} with uniformly sampled spanning trees T_1, \dots, T_s for a relatively small number of samples $s \ll |\mathbb{T}|$:

$$N_l \stackrel{(19)}{=} \sum_{T \in \mathbb{T}} \sum_{c \in C_l \cap C_T} \frac{1}{\rho_c |\mathbb{T}|} \approx \frac{|\mathbb{T}|}{s} \sum_{i=1}^s \sum_{c \in C_l \cap C_{T_i}} \frac{1}{\rho_c |\mathbb{T}|} = \frac{|\mathbb{T}|}{s} \frac{1}{|\mathbb{T}|} \sum_{i=1}^s \sum_{c \in C_l \cap C_{T_i}} \frac{1}{\rho_c} = \frac{1}{s} \sum_{i=1}^s \sum_{c \in C_l \cap C_{T_i}} \frac{1}{\rho_c} \quad (20)$$

In practice, we use the approximated occurrence probability $\tilde{\rho}_c$ instead of the exact occurrence probability ρ_c . This may introduce an additional source of variance or bias in the approximated number of cycles. In Section 8.1, we evaluate the strengths and drawbacks of this approximation.

6 An Approximate Algorithm for Sampling 2-Cells on a Graph

We now introduce the sampling algorithm that, given an overall probability P_l to sample a 2-cells of length l , returns a set \mathcal{C} of cells s.t. $\forall c \in C_l : P(c \in \mathcal{C}) \approx P_l |c|$.

For this, we sample s spanning trees as described above. Given the list of tuples $(u, v, \text{lca}(u, v), \tilde{\rho}_c)$ for each spanning tree T , we calculate $|c| = \text{depth}(u) + \text{depth}(v) - 2 \cdot \text{depth}(\text{lca}(u, v)) + 1$. Then, the algorithm selects each cell with probability q_c s.t. the overall probability is P_l . Each cycle c has an independent probability of $\rho_c q_c$ to be selected from each of the s spanning trees (and is only returned once if sampled multiple times). Hence we obtain the relationship:

$$P_l \stackrel{!}{=} 1 - (1 - \rho_c q_c)^s \approx \rho_c q_c s \quad \Leftrightarrow \quad q_c = \frac{1 - \sqrt[s]{1 - P_l}}{\rho_c} \approx \frac{P_l}{\rho_c s} \quad (21)$$

This equation only has a valid solution for $1 - \sqrt[s]{1 - P_l} < \rho_c$, i.e., only for sufficiently small target probabilities P_l or sufficiently large s . This is closely related to the practical limit that spanning trees have w.r.t. the cycle lengths they sample.

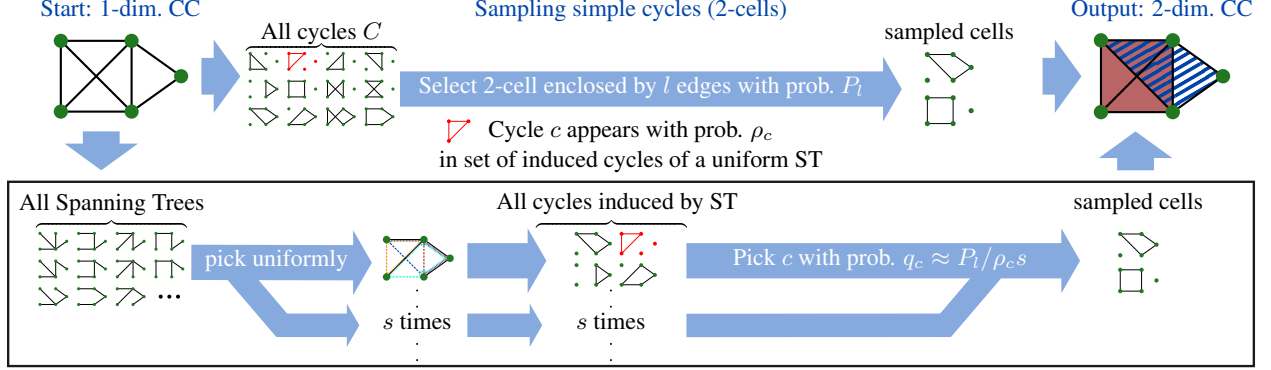


Figure 4: Random lifting from 1-dim. CC to 2-dim. CC and our sampling algorithm. The model (strong background colors) is simulated by dividing it into two steps (light background colors): First, s uniform spanning trees are sampled on the graph, each inducing a subset of all cycles. Depending on the probability ρ_c for any cycle to appear in such a subset, the cycles are then sampled as cells. The algorithm (boxes) closely follows the two-step sampling model, approximating ρ_c for efficiency.

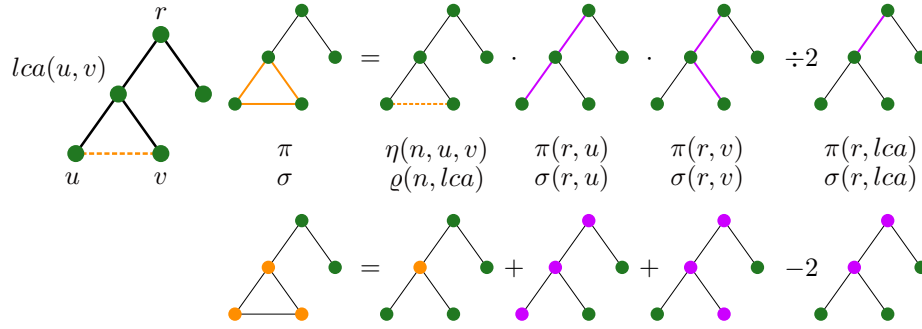


Figure 5: Illustration of the efficient calculation based on the tree structure.

7 Theoretical Considerations

In this section, we prove the algorithmic complexity of our spanning-tree-based cycle sampling approach and discuss theoretical limitations of spanning-tree-based sampling.

7.1 Algorithmic Complexity

Theorem 1. *On a graph sampled from an ER-model, our occurrence probability approximation takes $\mathcal{O}(s \cdot m^{1+\varepsilon})$.*

Proof. Without loss of generality, we assume that G is connected (otherwise, we execute the algorithm on each connected component separately). We can use Wilson's Algorithm [19] to efficiently sample spanning trees. Wilson's Algorithm is linear in the hitting time of the graph, i.e., the expected number of steps a random walk from any node to any other node takes. In the worst case, the hitting time is $\mathcal{O}(n^3)$ [23]. However, we are assuming the graph to be sampled from an ER model with probability p such that the resulting graph is almost surely connected as the number of nodes becomes large ($n \rightarrow \infty$). On these ER-Graphs, the hitting time is in $\mathcal{O}(n)$ [24].

Each spanning tree T induces a set of cycles C_T . Each cycle $c \in C_T$ is induced by a non-tree edge $(u, v) \in G \setminus T$ and consists of the edge (u, v) and the path $P_{u,v}$ from u to v in the tree. We split the calculation of Equation (11) into $\tilde{\rho}_c = \gamma(n, \tilde{d}, l) \cdot (\eta(n, u, v) + \sigma(u, v)) \cdot \pi(u, v)$, where $\sigma(u, v)$ denotes a sum and $\pi(u, v)$ a product over the path $P_{u,v}$. By defining $\sigma(u, v) = \sum_{(x,y) \in P_{u,v}} \eta(n, x, y)$ and $\pi(u, v) = \prod_{x \in P_{u,v}} \varrho(n, x)$, we retrieve $\tilde{\rho}_c$.

To calculate $\sigma(u, v)$ and $\pi(u, v)$ for all $u, v \in G$, we start at the root r and traverse the tree (cf. Figure 5). From the definition, $\pi(r, r) = \varrho(n, d(r))$, $\sigma(r, r) = 0$. For a node u with parent v , we calculate $\pi(r, u) = \pi(r, v) \cdot \varrho(n, d(u))$ and $\sigma(r, u) = \sigma(r, v) + \eta(d, u, v)$. Then, we can calculate $\sigma(u, v)$ and $\pi(u, v)$ for any $u, v \in G$ in constant time using the lowest common ancestor (lca) of u and v (cf. Equations (22) and (23) and Figure 5).

$$\pi(u, v) = \frac{\pi(r, u)\pi(r, v)\rho(n, d(\text{lca}(u, v)))}{\pi(r, \text{lca}(u, v))^2} \quad (22)$$

$$\sigma(u, v) = \sigma(r, u) + \sigma(r, v) - 2\sigma(r, \text{lca}(u, v)) + \eta(n, u, v) \quad (23)$$

We can calculate $\pi(r, u)$ and $\sigma(r, u)$ for all nodes u in $\mathcal{O}(n) \leq \mathcal{O}(m)$ by traversing the tree from the root downwards. Equations (22) and (23) have to be calculated only once for each edge that is not part of the tree, i.e., $\mathcal{O}(m)$. To compute the lowest common ancestor (lca) of two nodes, we use Tarjan’s off-line lca algorithm [25], which runs in $\mathcal{O}(n + m\alpha(n + m))$ (per tree), where α is the inverse of the Ackermann function. On a connected graph, the number of edges is, asymptotically, at least as large as the number of nodes, i.e., we can simplify the complexity of lca to $\mathcal{O}(m\alpha(2m)) \leq \mathcal{O}(m^{1+\varepsilon})$ for any $\varepsilon > 0$.

By multiplying with the number of sampled spanning trees s , the theorem follows. \square

Remark 1 (Complexity of calculating cycle lengths). *The length of the cycle induced by (u, v) is $\text{depth}(u) + \text{depth}(v) - 2 \cdot \text{depth}(\text{lca}(u, v)) + 1$. Calculating the depth of all nodes in a tree requires a traversal in $\mathcal{O}(n) \leq \mathcal{O}(m)$; for each cycle, the calculation takes constant time.*

Remark 2 (Complexity of sampling 2-cells). *For sampling 2-cells, in addition to the complexity analyzed above, we perform $\mathcal{O}(ms)$ calculations of q_c (and generate a random number for each); and enumerate the nodes of all chosen 2-cells.*

7.2 Theoretical Limitations

Aside from the accuracy of our approximation, our approach is also limited by properties of uniform spanning trees. To illustrate this, let us consider the complete graph K_n . On K_n , the prior estimation of the number of cycles \mathcal{N}_l and our approximated occurrence probability $\tilde{\rho}_c$ are exact. Overall, longer cycles are less frequently induced by a spanning tree (compare Figure 6a) despite being more numerous. In other words, longest paths on a uniform spanning tree are, with high probability, much shorter than the longest cycles on the graph. To a lesser extent, this also holds for ER-graphs (cf. Figure 6b).

Overcoming this would require an impractically large number of samples. In the worst case, the expected number of sampled cells c with length $l = n$ in one spanning tree is:

$$N_l \rho_c = \frac{n!}{(n-n)!} \frac{1}{2l} \cdot \frac{l}{1 + \frac{n-l}{n}} \frac{(n-2)^2}{n^{n-2}} = \frac{n!}{2} \frac{(n-2)^2}{n^{n-2}} \quad (24)$$

In other words, we would need to sample $\frac{1}{N_l \rho_c} \approx 2.2 \cdot 10^{34}$ spanning trees to get a single cycle for $n = l = 100$ in expectation.

In practice, this means that the cycles that we can sample are limited in length. For applications, we can choose to ignore cycles of lengths that do not appear often enough in the sampling process.

8 Empirical Evaluation

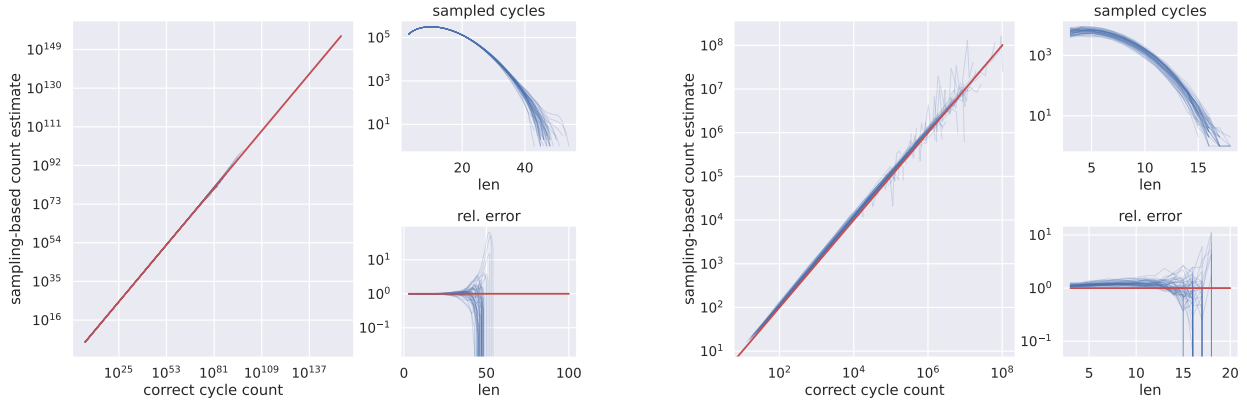
The evaluation code is available under github.com/josephhope/random-abstract-cell-complexes.

8.1 Approximation Accuracy

First, we compare our approximations of the occurrence probability $\tilde{\rho}_c$ on different configurations of Erdős–Rényi. Given a graph, we sample multiple spanning trees and calculate the occurrence probability ρ and our approximation $\tilde{\rho}_c$ for every cycle c induced by the spanning trees. Then, we repeat the procedure on other synthetic and real-world graphs to investigate the broader applicability of our approach to cycle sampling.

Figure 7 (a) shows that, given a sufficiently large number of nodes n and connection probability p , our approximation of ρ is very accurate. We can verify this by comparing to a simple baseline: Figure 13 shows predictions that are only based on the length of the cycle; which is considerably less accurate.

However, as Figure 7 (b) shows, for graphs that are relatively sparse, the accuracy drops. This is likely a result of graphs with smaller edge probabilities behaving more differently from the expected graph: Our approximation assumes a relatively densely and evenly connected graph. Sparse configurations of ER are more likely to deviate from this



(a) Cycle count estimation on the complete graph K_{100} ; 50 different runs shown.

(b) Cycle count estimation on 50 graphs sampled from ER with $n = 20, p = 0.3$.

Figure 6: The cycle count estimation \tilde{N}_l and the actual number of cycles N_l (red). With increasing l , cycles become less likely to be induced by a spanning tree. This results in a lower accuracy and estimates of $\tilde{N}_l = 0$ for larger l .

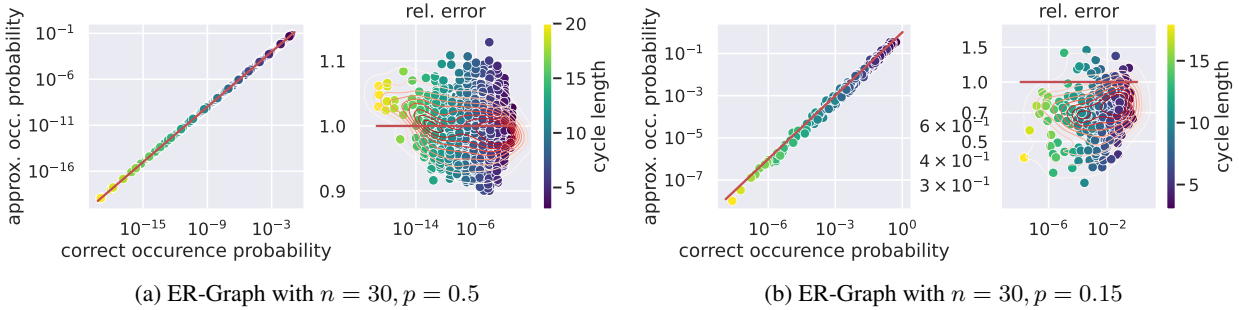


Figure 7: The approximated (b) occurrence probability $\tilde{\rho}_c$ of simple cycles on graphs sampled from ER; cycles for evaluation obtained from 10 uniform STs. On the denser ER-graph (a), the probabilities are approximated more accurately than on the sparser graph (b).

expectation than dense configurations: The degree distribution is less uniform and a (partial) path is more likely to ‘cut off’ parts of the graph due to the lower connectivity.

For graphs that are not sampled from the Erdős–Rényi model, the accuracy strongly depends on the structure. If the graph is globally and relatively evenly connected, the approximation is still accurate. We verified this with a number of synthetic examples in Figure 14 (a)–(e), where our approximation is fairly accurate on most graphs.

On graphs with a macro structure that is uneven, the accuracy drops dramatically. In a barbell graph (Figure 14 (f)), all cycles are contained in one of the complete subgraphs. However, the other nodes are still considered to be unvisited and possible neighbours, ultimately leading to an overestimation of the occurrence probability². The most notable exception is formed by planar networks, such as a Delaunay triangulation or grid graph (Figure 14 (g) and (h)). Here, we see a systematic underestimation of the occurrence probability for long cycles. This stems from the fact that the graph, while well-connected, has a large diameter and in nearly all steps, the target node is a neighbor with probability 0 instead of $1/n$. Theoretically, this should hold for all graphs where the local connectivity is significantly stronger than global connectivity. To a lesser degree, this can also be observed on the SBM (Figure 14 (c)), and likely many real-world networks.

Our experiments on synthetic graphs in Figure 15 support these results, with most graphs resulting in fairly small approximation errors. Graphs that have a comparatively large diameter or are (globally and nearly) planar show a systematic error, as indicated by our synthetic experiments.

²Through an underestimation of the connectedness to the target node: In reality, in every step, the target node is a neighbour, whereas our approximation approximates it to be a neighbour in every second step

8.2 Accuracy of Cycle Count Estimation

We evaluate the accuracy of the cycle count estimation by also calculating the correct number of cycles. For ER-Graphs, this means we have to choose small instances to sample from, making it possible to enumerate all cycles. Additionally, on the full graph, we can easily calculate the number of simple cycles, making it suitable for a comparison of the performance on larger graphs.

Given the good accuracy of the occurrence probability approximation, we expect the cycle count estimation to be similarly accurate, with the added condition that sufficiently many cells of the given length were induced by the sampled spanning trees. Figure 6b confirms this expectation, showing a slight overestimation for smaller lengths and a large increase in the error for longer cells. Furthermore, our experiments on the full graph (Figure 6a) show that the increase in error for longer cells is a result of the small number of sampled cycles since, on the full graph, all cells are the same and the estimated probability is always correct. This is exactly in line with our theoretical considerations.

8.3 Accuracy of Sampled Cell Count

Overall, the sampled number of cells that is very close to the desired number, as shown in Figure 18. Note that any skew of the occurrence probability results in an equal but opposite skew in the estimated number of cycles, leading in total to an accurate number of cells sampled.

8.4 Time Complexity

Figure 8 shows that our approach is highly scalable. Empirically, the runtimes for the approach are in line with our analysis as it takes approximately $\mathcal{O}(n^2)$, which is consistent with $\mathcal{O}(s \cdot m^{1+\epsilon})$ since $m \in \Theta(n^2)$ for a fixed p . We also evaluated the runtime on real-world networks (cf. Figure 11), which is practical to use even for networks with more than 10^7 edges. Furthermore, the algorithm is highly parallelizable as each spanning tree can be sampled from independently (which is not currently implemented).

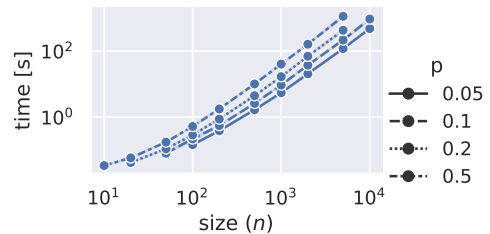


Figure 8: Runtime for $\nu = 10n$, $s = 1000$.

9 Properties of the Null Model

Before using the null model in applications, it is important to understand its basic properties. In this section, we explore the properties of the model, and, where applicable, compare to simplicial complexes that are generated from the same underlying graph.

First, in Figure 19b, we can see that most obtained CCs are not orientable, even with relatively few added cells. This is in contrast to SCs, which are orientable with considerably more added triangles, especially on triangulation graphs. Second, Figure 19a shows that in our experiments random CCs either have (almost) no 1-cohomology or (almost) no 2-cohomology. Simplicial complexes obtained on the same graphs often do not remove all 0-cohomologies; and are more limited in the number of 2-cohomologies they add. Since this depends on the density of triangles in the graph, this effect is especially pronounced on sparse random graphs and less or not present on dense graphs. Our model behaves similar on graphs obtained from point cloud triangulations. Due to the local structure, SCs can fill all 1-cohomologies, but add only few 2-cohomologies; they also remain orientable for many added triangles.

The spectrum of the Hodge Laplacian reflects the connectivity and structure of a cell complex. In Figure 9, we compare the largest eigenvalues of the up Laplacian L_1^{up} of the null model and the closest equivalent simplicial complex, i.e., uniformly adding triangles. We observe that the cell complex null model results in significantly larger eigenvalues, indicating more overlap between 2-cells and a closely-connected complex overall. When normalizing the up Laplacian to account for the boundary size of 2-cells, the gap between using triangles and using any other polygon increases in relative size. In other words, triangles capture the connectivity of the graph differently than any other polygons — namely, they capture *less* of the connectivity.

Both the homology and spectral analysis show a key shortcoming of approaches limited to triangles: On many graphs, triangles do not span the entire graph as they are usually concentrated in smaller cliques. Given that these properties are highly dependent on the underlying graph, these analyses only provide a first intuitive insight into random CCs. Thus, further theoretical analysis is required to fully understand the properties of random CCs.

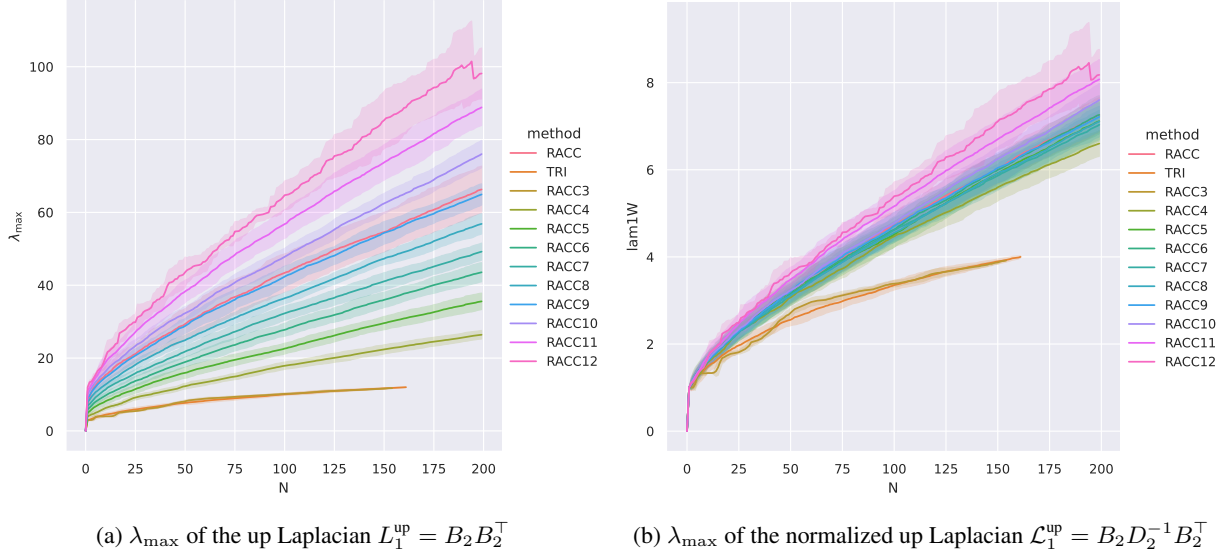


Figure 9: Biggest eigenvalues λ_{\max} of the up Laplacian (a) and normalized up Laplacian (b) of sampled CCs on an Erdős–Rényi Graph with $n = 20, p = 0.5$. In both figures, we compare our Model *RACC* to randomly selected triangles (*TRI*) and our model configured to only sample cells of length n (*RACCn*). We can see that the eigenvalue of our null model is significantly larger than that of *TRI*, even if we only sample cells with a boundary size of 4. To correct for the effect of the boundary size on the eigenvalue, we normalize the up Laplacian using the inverse of the degree matrix $D = B_2 \mathbb{1}$. The eigenvalue of the normalized up Laplacian still shows a large gap between triangles and larger 2-cells, indicating that larger 2-cells are able to capture structure that triangles cannot (on this graph).

10 Applications

In this section, we explore the use cases for random cell complexes we identified earlier. We focus on minimal examples showcasing the usage rather than a comprehensive analysis.

10.1 Null Model as Experiment Baseline

When evaluating novel methods that infer cells, it is useful to have a baseline that marks randomness. In the case of the flow representation learning problem [14], we see that random 2-cells are very inefficient in Figure 10. However, this also gives us a way to classify the performance of the approaches we want to evaluate. In this case, we see that the newly proposed methods give a representation that provides a significant improvement over *triangles*, but *triangles* is already a method that explains a lot of structure.

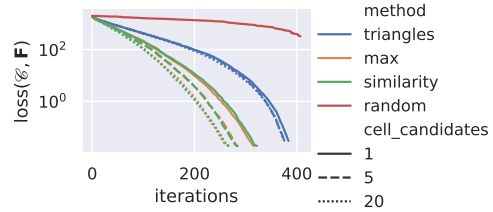


Figure 10: Comparison of the approaches to the flow representation learning problem from [14] and using random CCs (Anaheim dataset [26])³.

10.2 Sensitivity Analysis: How Important are Higher-Order Interactions?

In this section, we demonstrate the use of random CCs for the sensitivity (or ablation analysis [29]) of neural networks defined on higher-order networks.

In [17], Bodnar et al. propose a novel architecture for cell complex neural networks (CWNs). To obtain a cell complex and capture structural information on a graph, they add chordless cycles as 2-cells. On the synthetic *RingTransfer* benchmark, the authors demonstrate that 2-cells also improve the propagation of node features. Here we use our random cell complex model to investigate in how far this specific choice of 2-cells is relevant or if adding random cells would have yielded similar results. This provides insights into whether it is the *specific* cell structure (adding chordless cycles)

³Code available at github.com/josephoppe/random-abstract-cell-complexes.

that conveys an advantage, or whether it is merely the increase in expressive power of the neural networks (resulting from adding higher-order cells) that is of importance.

Interestingly, for the PROTEINS dataset (see Table 1) there is no significant performance difference if we simply add random 2-cells instead of following the procedure outlined in [17]. Indeed, a similar performance can even be gained by not adding any 2-cells at all. In contrast, on the NCI109 dataset [27], adding random 2-cells significantly decrease the accuracy. This observation indicates that the 2-cell lifting procedure proposed in [17] works as intended on NCI109, but fails to capture relevant topological information on PROTEINS beyond what we could expect by simply increasing the expressivity of the network. To corroborate our findings, we have added a further comparison to the PPGN architecture [28]. PPGN also features an increased expressivity compared to standard GNNs, but is not based on any topological considerations. As Table 1 shows PPGN works well in the PROTEIN dataset, yet only performs as good as adding random cells in CWN. In conclusion, this example hints at how random cell complexes can lead to further insights into what features drive the performance of higher-order GNNs.

Table 1: Comparison of CWN [17] with the original 2-cells ('Rings'), random 2-cells ('RND'), and no 2-cells ('None'). Code available at github.com/josefhoppe/cwn-random-ccs. Results deviate slightly from [17] despite using the original code. Accuracy of PPGNs from [17].

DATASET [27]	PROTEINS	NCI109
CWN (RINGS)	73.8 ± 4.3	84.5 ± 1.6
CWN (RND)	74.2 ± 5.0	82.2 ± 1.3
CWN (NONE)	73.0 ± 5.5	82.9 ± 1.2
PPGNs [28]	77.2 ± 4.7	82.2 ± 1.4

11 Conclusion

The main contributions of this paper are (i) the introduction of a simple model for random abstract cell complexes, (ii) a general approach to working with the set of simple cycles on a graph, (iii) an efficient approximate sampling algorithm for the model, and (iv) a cycle count estimation algorithm required to make the model more amenable to application scenarios, in which we want to fix the number of sampled cells in expectation. We explored some properties of this model and showcased how it enables a number of investigations concerning higher-order network data and learning methods operating with such data: Specifically, random CCs can be used as synthetic input data and as null models for multiple purposes.

This groundwork opens up multiple avenues for future research on abstract cell complexes: First, a more theoretical analysis of the number of simple cycles and the behavior of RCCs. Second, while we defined our model for arbitrary dimensions, higher-dimensional cells add considerable combinatorial complexity, which is why we limited our sampling algorithm to 2-cells. Indeed, adapting our sampling algorithm to higher-order cells is not trivial as the higher-dimensional analogues of spanning trees do not share many of their desirable properties.

When employing random cell complexes as synthetic data, it may also be desirable to include more structure in the cell complexes, both on the edge and cell levels. On the level of 2-cells, a simple extension could introduce a block structure and modify the sampling probabilities based on block membership.

Finally, the approach to explore the cycle space using spanning trees is applicable beyond higher-order networks. Any graph property that can be calculated over cycles on a graph can be approximated using our sampling-based approximation. This includes direct analysis of network properties, but can also yield features, for example for graph learning.

Acknowledgements

Funded by the European Union (ERC, HIGH-HOPeS, 101039827). Views and opinions expressed are however those of the author(s) only and do not necessarily reflect those of the European Union or the European Research Council Executive Agency. Neither the European Union nor the granting authority can be held responsible for them.

References

- [1] Paul Erdős and Alfréd Rényi, "On random graphs I," *Publ. math. debrecen*, vol. 6, no. 290-297, pp. 18, 1959.
- [2] Réka Albert and Albert-László Barabási, "Statistical mechanics of complex networks," *Reviews of modern physics*, vol. 74, no. 1, pp. 47, 2002.
- [3] Mikhail Drobyshvskiy and Denis Turdakov, "Random graph modeling: A survey of the concepts," *ACM computing surveys (CSUR)*, vol. 52, no. 6, pp. 1–36, 2019.

- [4] Edgar N Gilbert, “Random graphs,” *The Annals of Mathematical Statistics*, vol. 30, no. 4, pp. 1141–1144, 1959.
- [5] Paul W Holland, Kathryn Blackmond Laskey, and Samuel Leinhardt, “Stochastic blockmodels: First steps,” *Social networks*, vol. 5, no. 2, pp. 109–137, 1983.
- [6] Bailey K Fosdick, Daniel B Larremore, Joel Nishimura, and Johan Ugander, “Configuring random graph models with fixed degree sequences,” *Siam Review*, vol. 60, no. 2, pp. 315–355, 2018.
- [7] Christian Bick, Elizabeth Gross, Heather A Harrington, and Michael T Schaub, “What are higher-order networks?,” *SIAM Review*, vol. 65, no. 3, pp. 686–731, 2023.
- [8] Leo Torres, Ann S Blevins, Danielle Bassett, and Tina Eliassi-Rad, “The why, how, and when of representations for complex systems,” *SIAM Review*, vol. 63, no. 3, pp. 435–485, 2021.
- [9] Federico Battiston, Giulia Cencetti, Iacopo Iacopini, Vito Latora, Maxime Lucas, Alice Patania, Jean-Gabriel Young, and Giovanni Petri, “Networks beyond pairwise interactions: Structure and dynamics,” *Physics Reports*, vol. 874, pp. 1–92, 2020.
- [10] Larry Wasserman, “Topological data analysis,” *Annual Review of Statistics and Its Application*, vol. 5, pp. 501–532, 2018.
- [11] Sergio Barbarossa and Stefania Sardellitti, “Topological signal processing over simplicial complexes,” *IEEE Transactions on Signal Processing*, vol. 68, pp. 2992–3007, 2020.
- [12] Michael T Schaub, Yu Zhu, Jean-Baptiste Seby, T Mitchell Roddenberry, and Santiago Segarra, “Signal processing on higher-order networks: Livin’ on the edge... and beyond,” *Signal Processing*, vol. 187, pp. 108149, 2021.
- [13] Mustafa Hajij, Ghada Zamzmi, Theodore Papamarkou, Nina Miolane, Aldo Guzmán-Sáenz, Karthikeyan Natesan Ramamurthy, Tolga Birdal, Tamal K Dey, Soham Mukherjee, Shreyas N Samaga, et al., “Topological deep learning: Going beyond graph data,” *arXiv preprint arXiv:2206.00606*, 2022.
- [14] Josef Hoppe and Michael T. Schaub, “Representing Edge Flows on Graphs via Sparse Cell Complexes,” in *The Second Learning on Graphs Conference*, 2023.
- [15] Nathan Linial* and Roy Meshulam*, “Homological connectivity of random 2-complexes,” *Combinatorica*, vol. 26, no. 4, pp. 475–487, 2006.
- [16] Armindo Costa and Michael Farber, “Random simplicial complexes,” in *Configuration Spaces: Geometry, Topology and Representation Theory*, pp. 129–153. Springer, 2016.
- [17] Cristian Bodnar, Fabrizio Frasca, Nina Otter, Yuguang Wang, Pietro Lio, Guido F Montufar, and Michael Bronstein, “Weisfeiler and lehmman go cellular: Cw networks,” *Advances in Neural Information Processing Systems*, vol. 34, pp. 2625–2640, 2021.
- [18] Maciej Marek Sysło, “On cycle bases of a graph,” *Networks*, vol. 9, no. 2, pp. 123–132, 1979.
- [19] David Bruce Wilson, “Generating random spanning trees more quickly than the cover time,” in *Proceedings of the twenty-eighth annual ACM symposium on Theory of computing*, 1996, pp. 296–303.
- [20] JW Lyklema, Carl Everts, and L Pietronero, “The laplacian random walk,” *Europhysics Letters*, vol. 2, no. 2, pp. 77, 1986.
- [21] Josef Hoppe, Vincent P. Grande, and Michael T. Schaub, “Don’t be Afraid of Cell Complexes! An Introduction from an Applied Perspective,” 2025, arXiv Preprint. arXiv:2506.09726.
- [22] Surya T Tokdar and Robert E Kass, “Importance sampling: a review,” *Wiley Interdisciplinary Reviews: Computational Statistics*, vol. 2, no. 1, pp. 54–60, 2010.
- [23] Graham Brightwell and Peter Winkler, “Maximum hitting time for random walks on graphs,” *Random Structures & Algorithms*, vol. 1, no. 3, pp. 263–276, 1990.
- [24] Matthias Löwe and Felipe Torres, “On hitting times for a simple random walk on dense erdős–rényi random graphs,” *Statistics & Probability Letters*, vol. 89, pp. 81–88, 2014.
- [25] Robert Endre Tarjan, “Applications of path compression on balanced trees,” *Journal of the ACM (JACM)*, vol. 26, no. 4, pp. 690–715, 1979.
- [26] Transportation Networks for Research Core Team, “Transportation networks for research,” 2020, Accessed: 2024-01-29.
- [27] Christopher Morris, Nils M Kriege, Franka Bause, Kristian Kersting, Petra Mutzel, and Marion Neumann, “TUDataset: A collection of benchmark datasets for learning with graphs,” *arXiv preprint arXiv:2007.08663*, 2020.

-
- [28] Haggai Maron, Heli Ben-Hamu, Hadar Serviansky, and Yaron Lipman, “Provably powerful graph networks,” *Advances in neural information processing systems*, vol. 32, 2019.
- [29] Chris Fawcett and Holger H Hoos, “Analysing differences between algorithm configurations through ablation,” *Journal of Heuristics*, vol. 22, pp. 431–458, 2016.
- [30] Pim van der Hoorn, Gabor Lippner, and Dmitri Krioukov, “Sparse maximum-entropy random graphs with a given power-law degree distribution,” *Journal of Statistical Physics*, vol. 173, pp. 806–844, 2018.
- [31] Duncan J Watts and Steven H Strogatz, “Collective dynamics of ‘small-world’ networks,” *nature*, vol. 393, no. 6684, pp. 440–442, 1998.
- [32] Jesper Dall and Michael Christensen, “Random geometric graphs,” *Physical review E*, vol. 66, no. 1, pp. 016121, 2002.
- [33] Matthew Kahle, “Topology of random clique complexes,” *Discrete mathematics*, vol. 309, no. 6, pp. 1658–1671, 2009.
- [34] Matthew Kahle et al., “Topology of random simplicial complexes: a survey,” *AMS Contemp. Math*, vol. 620, pp. 201–222, 2014.
- [35] Martina Zähle, “Random cell complexes and generalised sets,” *The Annals of Probability*, pp. 1742–1766, 1988.
- [36] Benjamin Schweinhart, Jeremy K Mason, and Robert D MacPherson, “Topological similarity of random cell complexes and applications,” *Physical Review E*, vol. 93, no. 6, pp. 062111, 2016.
- [37] Lutz Leistritz and Martina Zähle, “Topological mean value relations for random cell complexes,” *Mathematische Nachrichten*, vol. 155, no. 1, pp. 57–72, 1992.
- [38] Chris Whong, “FOILing NYC’s Taxi Trip Data,” 2014, chriswhong.com/open-data/foil_nyc_taxi. Accessed 2024-03-28.
- [39] Stefania Sardellitti, Sergio Barbarossa, and Lucia Testa, “Topological signal processing over cell complexes,” in *2021 55th Asilomar Conference on Signals, Systems, and Computers*. IEEE, 2021, pp. 1558–1562.
- [40] Robin Pemantle, “Choosing a Spanning Tree for the Integer Lattice Uniformly,” *The Annals of Probability*, pp. 1559–1574, 1991.
- [41] Oded Schramm, “Scaling limits of loop-erased random walks and uniform spanning trees,” *Israel Journal of Mathematics*, vol. 118, no. 1, pp. 221–288, 2000.
- [42] Wayne W Zachary, “An Information Flow Model for Conflict and Fission in Small Groups,” *Journal of Anthropological Research*, vol. 33, no. 4, pp. 452–473, 1977.
- [43] CJ Rhodes and P Jones, “Inferring missing links in partially observed social networks,” *Journal of the operational research society*, vol. 60, no. 10, pp. 1373–1383, 2009.

A Related Work

Random graph models. Random graph models started with the Erdős–Rényi random graph model [1], which originally proposed to draw a graph uniformly at random from the set of all graphs with a fixed number of nodes and edges. In this paper, we refer to a variant introduced by Gilbert [4] but commonly also referred to as Erdős–Rényi model, that draws each edge independently with probability p . More complex graph models generally focus on modeling community structure (most notably the Stochastic Block Model [5]) or the distribution of node degrees [2, 30]. Furthermore, there are models aimed to more closely approximate real-world networks, such as the Watts–Strogatz small-world graph [31], modeling the small diameter of real-world networks. Finally, graphs may be generated from random point clouds by connecting nodes that are close to each other in metric space [32]; resulting in the formation of clusters similar to real-world networks. There are many more models and ways to configure models that would exceed the scope of this literature review, but it should be noted that many use cases for these models exist, requiring different graph models.

Random simplicial complex models. The Linial-Meshulam model for random SCs [15] is an extension of Erdős–Rényi to higher dimensions. LM takes a complete $(d - 1)$ -dimensional complex and samples i.i.d. from all possible d -simplices. The Linial-Meshulam model was generalized in multiple ways, e.g. a different static probability P_d to sample d -simplices (separately) for each dimension (i.e., cardinality) d [16]. In a similar vein to our model, random clique complexes [33], i.e., SCs obtained by adding all cliques of a random graph as simplices, build on a graph as a 1-skeleton. We refer to [34, 16] for a more detailed overview of existing models. To date, no SC model analogues to many of the well-known random graph models (e.g. modeling community structure, degree distribution, etc.) exist.

Random (abstract or geometric) cell complex models. On a theoretical level, random cell complexes in high-dimensional euclidean spaces were introduced by [35]. This results in geometric cell complexes, i.e., cell complexes that have an embedding and a distinction between cells that lie on the inside of the complex and those on the outside. Moreover, to the best of our knowledge, there is no known efficient algorithm to sample from this distribution. Further research on random geometric cell complexes [36, 37] focused on tessellations of low- or high-dimensional point clouds and the local topology characterizing physical cell complexes. Such geometric graphs (or CCs) may accurately model some real-world datasets (e.g., communication between internet nodes) as they result in sparse, planar graphs with a possibly quite large diameter. However, many applications have more dense, non-planar graphs with small diameters, such as telecommunication between cell towers [11], taxi trips (by endpoints) between neighborhoods [38], or social networks. To date, researchers have filled the gaps in both models and sampling algorithms for existing models by using simple lifting procedures, lifting a well-structured graph to an abstract cell complex, or using a possibly biased sampling method. Limiting the lifting to chordless cycles up to a certain length, for example, makes it computationally feasible to compute all possible 2-cells (in practice) [17]. Alternatively, cells can be sampled from the Delaunay triangulation of a two-dimensional point cloud [14, 39]. However, these are ad hoc constructions to provide a useful lifting for certain datasets or synthetic data for an evaluation, respectively. These methods have geometric properties and have not been studied in detail; they may therefore introduce biases into the resulting data: For example, [14] uses a process that consecutively augments triangles with neighboring triangles. This growth process necessarily stops at the outer edges of the triangulation, making them more likely to be part of a cell boundary than inner edges. The usage of these ad hoc models clearly indicates the need for models of random abstract cell complexes.

B Approximation of the Occurrence Probability ρ_c

A cycle is induced by a spanning tree if and only if all but one of its edges are part of a spanning tree. Each path formed by removing an edge from the cycle has a certain probability of being part of the spanning tree. By summing these probabilities, we can obtain the overall occurrence probability ρ_c .

To approximate this, we briefly outline at the loop-erased random walk that is also used to sample uniform spanning trees. Then, we present the Laplacian Random Walk [20], a different formulation that has the same probability as the loop-erased random walk. This gives an exact equation for the occurrence probability ρ_c . Finally, we introduce an approximation of that equation that can be calculated efficiently on spanning trees.

B.1 The Loop-Erased Random Walk

On a graph G , a loop-erased random walk from node u to node v can be obtained by performing a regular random walk and, whenever it self-intersects, removing the loop that formed from the self-intersection. Wilson’s Algorithm [19] for uniform spanning trees performs a series of loop-erased random walks, each adding edges until a spanning tree is found.

It is no surprise, then, that the distribution of loop-erased walks from node u to node v on a graph G is the same as the distribution of the path between u and v on a uniformly sampled spanning tree $T \subseteq G$ [40].

B.2 The Laplacian Random Walk

The Laplacian Random Walk (LRW) [20] from u to v has the same probability distribution as the loop-erased random walk from u to v [41]. The LRW achieves the same probability distribution as the loop-erased random walk by avoiding loops in the first place. To do this, the transition probabilities have to be adjusted to account for the possibility of creating a loop before reaching the target node v . First, nodes that were already visited are never chosen. Second, nodes with no connection to the target node (except through the current node or previously visited nodes) are also never chosen as the LRW would have to return to a visited node before reaching the target node. Intuitively, the probability of all other nodes is adjusted to account for the probability of a loop-erased random walk closing a loop.

In every step of the LRW, the set of already visited nodes changes, thus necessitating a recalculation of these probabilities. The probabilities can be modeled using the Graph Laplace operator $L = D - A$: In each step i , the LRW defines a function $f_i : V \rightarrow \mathbb{R}$ on the nodes. For the target node v , it has a fixed value of $f_i(v) = 1$. Conversely, all nodes w already visited at time i have a fixed value of $f_i(w) = 0$. For all other nodes w , the probabilities are the solution to $L(f_i)(w) = 0$, i.e., their value is the average of their neighbors. The probability to transition from u to w is then $\tau^{(i)}(w) = f_i(w) / \sum_{x \in \text{Neigh}(u)} f_i(x)$. The probability density f_i depends on the visited nodes, and, consequently, so does the transition probability $\tau^{(i)}$.

B.3 Calculating the Occurrence Probability and Approximating the Laplacian Random Walk

As discussed, a spanning tree induces a cycle c if and only if all but one edge of c are part of the tree. The probability of each of these paths being part of the tree can be calculated using the laplacian random walk: For every edge (u, v) in c , we calculate the LRW probability of the path $c \setminus \{(u, v)\}$.

$$\rho_c = \sum_{(u,v) \in c} \prod_{i=1}^{|c|-1} \tau_i(c_{i+1}) = \sum_{(u,v) \in c} \prod_{i=1}^{|c|-1} \frac{f_i(c_{i+1})}{\sum_{y \in \text{Neigh}(c_i)} f_i(y)} \quad (25)$$

Since the LRW requires calculating f_i for every step of the walk, it is too computationally expensive for our purpose. To efficiently approximate this, we use the expected graph for our calculations. The expected ER graph is a weighted complete graph with a weight of p on each edge. All nodes that have not been visited and are not v or adjacent to it are symmetric (including weights). Thus, their \tilde{f}_i will be the same, meaning only the number of visited nodes i influence this. This gives us the following estimation:

$$\forall u : f_i(u) \approx \begin{cases} 1 & \text{if } u \text{ is the target} \\ 0 & \text{if } u \text{ has been visited} \\ \tilde{f}_i := \frac{i \cdot 0 + 1 \cdot 1}{i+1} = \frac{1}{i+1} & \text{else} \end{cases} \quad (26)$$

For nodes that are adjacent to the current node, we can give a more accurate approximation. The current node is adjacent and, by definition, has value 0, reducing the expectation of f_i . While this is symmetric for unvisited neighbors, the target node may also be a neighbor (with some probability). Thus, the transition probability to the correct next node is smaller than $\exp f_i$ suggests.

To retrieve a uniform value, we approximate the degree of the neighbor $d(x)$ with the mean degree \tilde{d} . For a neighbor node x , we approximate $f_i(x) \approx \tilde{f}'_i$:

$$\tilde{f}'_i = \frac{\overbrace{0 \cdot 1}^{\text{cur. node}} + \overbrace{d(x) - 1}^{\text{other neigh.}} \overbrace{0 \cdot (i-1)}^{\text{other visited}} + \overbrace{1 \cdot 1}^{\text{target } v} + \overbrace{\tilde{f}_i \cdot (n-i-2)}^{\text{unvisited}}}{\tilde{d}} \quad (27)$$

$$= \frac{\tilde{d} - 1}{\tilde{d}} \frac{1 + \frac{n-i-2}{i+1}}{n-2} \quad (28)$$

$$= \frac{\tilde{d} - 1}{\tilde{d}} \frac{n-1}{n-2} \frac{1}{i+1} \quad (29)$$

Furthermore, for the penultimate node, we know that one of the neighbors is the target node v . Thus, its f_{l-2} is bigger, increasing the probability for this step. We call it \tilde{f}_{l-2}'' :

$$\tilde{f}_{l-2}'' = \frac{\overbrace{0 \cdot 1}^{\text{cur. node}} + \overbrace{1 \cdot 1}^{\text{target } v} + \overbrace{\tilde{d} - 2}^{\text{exp. neigh.}} + \overbrace{0 \cdot (l-3)}^{\text{other vis.}} + \overbrace{\tilde{f}_{l-2} \cdot (n-l)}^{\text{unvisited}}}{\tilde{d}} \quad (30)$$

$$= \frac{1 + \frac{\tilde{d}-2}{n-3} \frac{n-l}{l-1}}{\tilde{d}} \quad (31)$$

With these considerations, we can approximate the probabilities $\tau_c^{(i)}$ of individual steps of the LRW. For the first step, no other node has been visited and all neighbors are either unvisited or v . Since the first step only depends on the size of the graph n , the mean degree \tilde{d} , and the degree of the first node d , we will denote it as $\tilde{\tau}_c^{(1)}(n, d)$. We know that one of our neighbors is the target node v as the edge (u, v) closes the cycle. The remaining $d-1$ neighbors, including the next node, are unvisited.

$$\tilde{\tau}_c^{(1)}(n, d, \tilde{d}) = \frac{\tilde{f}'_1}{1 + (d-1)\tilde{f}'_1} \quad (32)$$

$$= \frac{1}{\tilde{f}'_1^{-1} + d - 1} \quad (33)$$

$$= \frac{1}{2 \frac{\tilde{d}}{d-1} \frac{n-2}{n-1} + d - 1} \quad (34)$$

For the intermediate steps $i = 2, \dots, l-2$, we can derive a similar formula. This $\tilde{\tau}_c^{(i)}(n, d, i)$ also depends on the step i in the random walk. Note that we already know that one neighbor has been visited in the previous step, so we only need to consider the remaining $d-1$ neighbors, one of which is the next node in the walk. Of these, in expectation, $\frac{i-2}{n-2}$ have been visited so far and $\frac{1}{n-2}$ neighbors are the target node v . $\frac{n-i-1}{n-2}$ are unvisited.

$$\tilde{\tau}_c^{(i)}(n, d, i) = \frac{\tilde{f}'_i}{\tilde{f}'_i + (d-2) \frac{1}{n-3} ((n-i-2)\tilde{f}'_i + 1)} \quad (35)$$

$$= \frac{1}{1 + (d-2) \frac{1}{n-3} (n-i-2 + \tilde{f}'_i^{-1})} \quad (36)$$

However, this is difficult to compute as it depends on i , thus, we will derive a further approximation $\tilde{\tau}_c^{(i)}(n, d)$ that does not depend on i by approximating $\tilde{f}'_i \approx \tilde{f}_i$. This introduces a systematic error that we will correct afterwards by multiplying with the quotient of the more accurate and less accurate version using the expected degree of all nodes.

$$\tilde{\tau}_c^{(i)}(n, d) = \frac{\tilde{f}_i}{\tilde{f}_i + (d-2) \frac{1}{n-3} ((n-i-2)\tilde{f}_i + 1)} \quad (37)$$

$$= \frac{1}{1 + (d-2) \frac{1}{n-3} (n-i-2 + \tilde{f}_i^{-1})} \quad (38)$$

$$= \frac{1}{1 + (d-2) \frac{1}{n-3} (n-i-2 + i + 1)} \quad (39)$$

$$= \frac{1}{1 + (d-2) \frac{n-1}{n-3}} \quad (40)$$

For the transition in step $l-2$, where v is a neighbor of the next node on the walk, we can give a more accurate approximation as well. Since $\tilde{\tau}_c^{(l-2)}(n, d, l)$ depends on l , we will also only use the expected value for a correction.

$$\tilde{\tau}_c^{(l-2)}(n, d, l) = \frac{\tilde{f}_{l-2}''}{\tilde{f}_{l-2}'' + (d-2)\frac{1}{n-3}((n-(l-2)-2)\tilde{f}_{l-2} + 1)} \quad (41)$$

$$= \frac{\tilde{f}_{l-2}''}{\tilde{f}_{l-2}'' + (d-2)\frac{1}{n-3}((n-l)\tilde{f}_{l-2} + 1)} \quad (42)$$

For the transition $\tau_c^{(l-1)}(n, d, l)$ to v (step $l-1$), we know that v is a neighbor. Therefore, there is one neighbor that was certainly visited, one that has value 1, and of the remaining $d-2$ neighbors, $\frac{n-(l-1)-1}{n-3} = \frac{n-l}{n-3}$ have not been visited and have value f_{l-1} :

$$\tilde{\tau}_c^{(l-1)}(n, d, l) = \frac{1}{1 + (d-2)\frac{n-l}{n-3}f_{l-1}} \quad (43)$$

Overall, we can then approximate the occurrence probability of a cycle c with length $l > 3$. We use $E(\cdot)$ to denote the expected value, i.e., calculated using exact i and l , but the expected (mean) degree \tilde{d} instead of the correct node degree. For better readability, we divide the formula into a correctional part $\gamma(n, \tilde{d}, l)$, a sum part $\eta(n, u, v)$, and a product part $\varrho(n, u)$.

Equation (44) supposes an arbitrary but fixed direction over the open paths of the cycle. For the exact occurrence probability, the direction does not change the probability. For our approximation, it may however lead to small differences. Furthermore, when calculating the probability, there will not be a consistent direction. Thus, we symmetrize the probability by taking the average over both directions in Equation (45).

$$\rho_c \approx \tilde{\rho}_c = \sum_{(u,v),(v,w),(w,x) \in c} \tilde{\tau}_c^{(l-1)}(n, d(w), l) \tilde{\tau}_c^{(l-2)}(n, d(x), l) \tilde{\tau}_c^{(1)}(n, d(u), \tilde{d}) \prod_{i=2}^{l-3} \tilde{\tau}_c^{(i)}(n, d(c_{u+i}), i) \quad (44)$$

$$\approx \tilde{\rho}_c = \left(\prod_{i=2}^{l-2} \frac{E(\tilde{\tau}_c^{(i)})}{E(\tilde{\tau}_c^{(i)})} \right) \frac{E(\tilde{\tau}_c^{(l-2)})}{E(\tilde{\tau}_c^{(i)})} \frac{E(\tilde{\tau}_c^{(l-1)})}{E(\tilde{\tau}_c^{(i)})} \left(\sum_{(u,v) \in c} \frac{\tilde{\tau}_c^{(1)}(n, d(u), \tilde{d}) + \tilde{\tau}_c^{(1)}(n, d(v), \tilde{d})}{2\tilde{\tau}_c^{(i)}(n, d(u))\tilde{\tau}_c^{(i)}(n, d(v))} \right) \prod_{u \in c} \underbrace{\tilde{\tau}_c^{(i)}(n, d(u))}_{\varrho(n, u)} \quad (45)$$

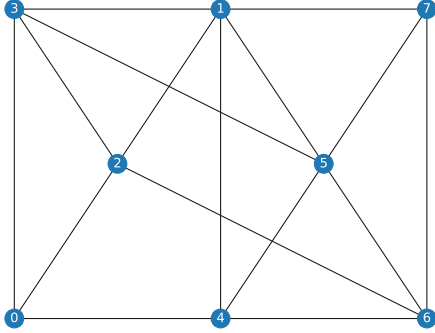
$$= \underbrace{\left(\prod_{i=2}^{l-2} \frac{\tilde{\tau}_c^{(i)}(n, \tilde{d}, i)}{\tilde{\tau}_c^{(i)}(n, \tilde{d})} \right)}_{\gamma(n, \tilde{d}, l)} \frac{\tilde{\tau}_c^{(l-2)}(n, \tilde{d}, l)}{\tilde{\tau}_c^{(i)}(n, \tilde{d})} \frac{\tilde{\tau}_c^{(l-1)}(n, \tilde{d}, l)}{\tilde{\tau}_c^{(i)}(n, \tilde{d})} \left(\sum_{(u,v) \in c} \eta(n, u, v) \right) \prod_{u \in c} \varrho(n, u) \quad (46)$$

$$= \gamma(n, \tilde{d}, l) \left(\sum_{(u,v) \in c} \eta(n, u, v) \right) \prod_{u \in c} \varrho(n, u) \quad (47)$$

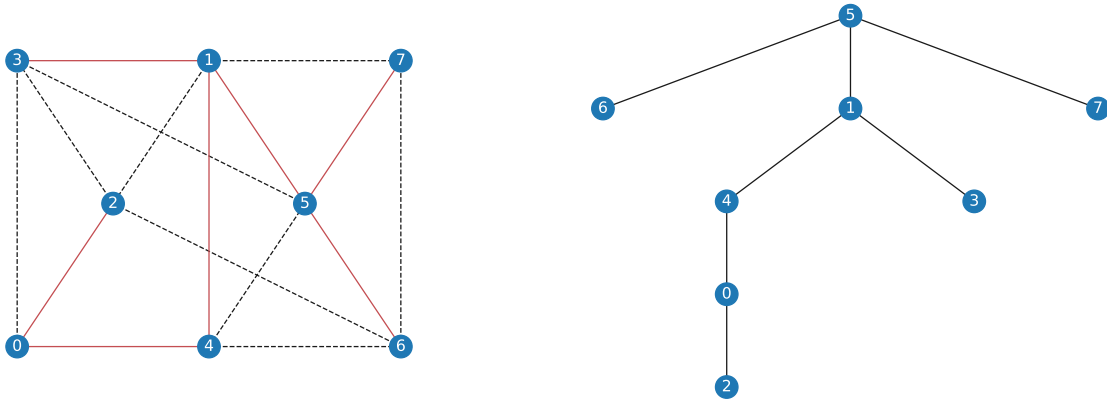
As discussed in Section 7.1, this approximation can be efficiently calculated using a spanning tree.

C Example Run on Toy Graph

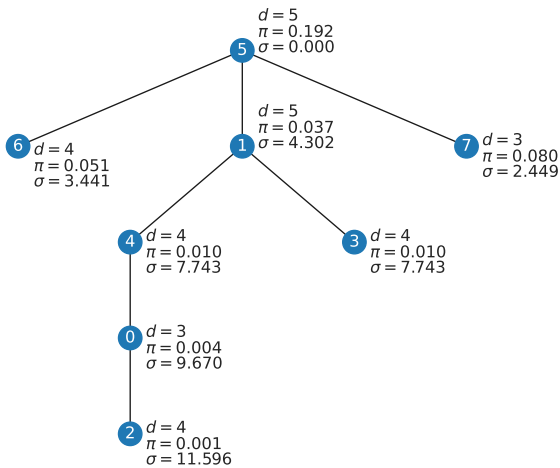
This section provides an example run to give a better intuition on how the algorithm and its optimizations work. We will be using the following graph drawn from Erdős–Rényi ($n = 8, p = 0.5$):



First, we sample a uniform spanning tree (left: highlighted on graph, right: displayed as rooted spanning tree).



As explained in Section 7.1, we can calculate $\tilde{\rho}_c$ for all cycles $c \in C_T$ efficiently. For this, we calculate $\sigma(r, u), \pi(r, u)$ for all $u \in T$:



Then, we calculate all lowest common ancestors using Tarjan’s off-line lca algorithm [25]. In our example, we will look at the edge $(0, 3)$ with $\text{lca}(0, 3) = 1$. The corresponding cycle is $c = (0, 3, 1, 4)$; we can compute its length without iterating it from the height of u, v , and their lowest common ancestor in the tree.

From this information, we can calculate $\tilde{\rho}_c$ by evaluating Equations (22) and (23):

$$\pi(0, 3) = \frac{\pi(r, 0)\pi(r, 3)\varrho(n, d(\text{lca}(u, v)))}{\pi(r, \text{lca}(u, v))^2} = \frac{0.0041 \cdot 0.0097 \cdot 0.19}{0.037^2} = 0.0055 \tag{48}$$

$$\sigma(0, 3) = \sigma(r, 0) + \sigma(r, 3) - 2\sigma(r, \text{lca}(0, 3)) = 9.67 + 7.74 - 2 \cdot 4.30 + 1.93 = 8.81 \tag{49}$$

$$\tilde{\rho}_c = \gamma(n, \tilde{d}, l) \cdot (\eta(n, 0, 3) + \sigma(0, 3)) \cdot \pi(0, 3) = 3.28 \cdot (1.93 + 8.81) \cdot 0.0055 = 0.195 \tag{50}$$

For comparison, the exact occurrence probability is $\rho_c = 0.210$.

D Additional Plots

The evaluation code used to generate these plots is available at github.com/josefhoppe/random-abstract-cell-complexes.

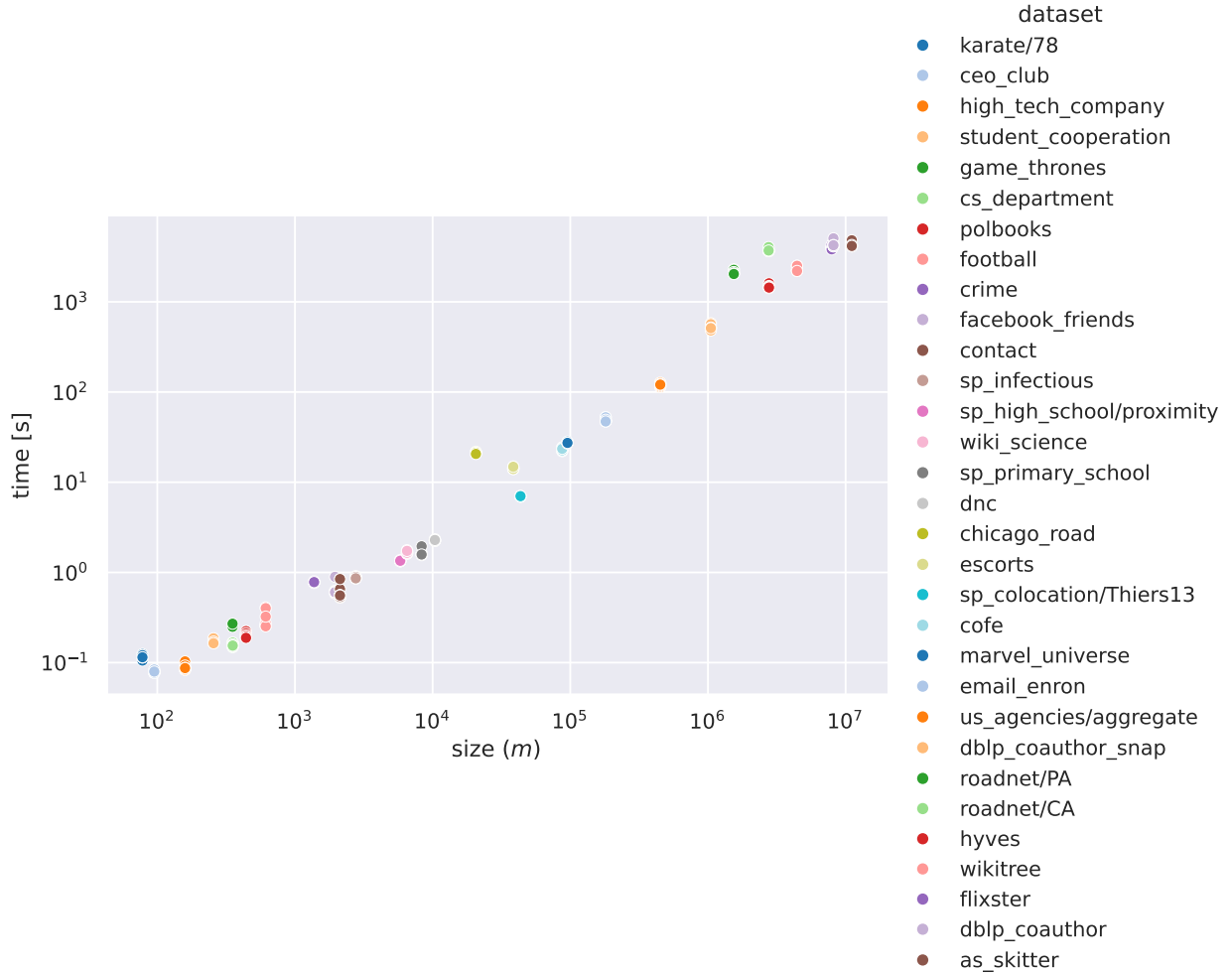


Figure 11: Runtime on selected real-world datasets (retrieved from *Netzschleuder*, <https://networks.skewed.de>, same naming convention), ordered by number of edges (m); $\nu = n$ sampled 2-cells from 1000 sampled trees; ten runs per graph. For disconnected networks, we used the largest connected component. The sample includes some of the largest networks available on *Netzschleuder*. This shows that our algorithm is performant enough for practical applications on a large number of real-world datasets. On larger datasets, the performance may not as practically applicable.

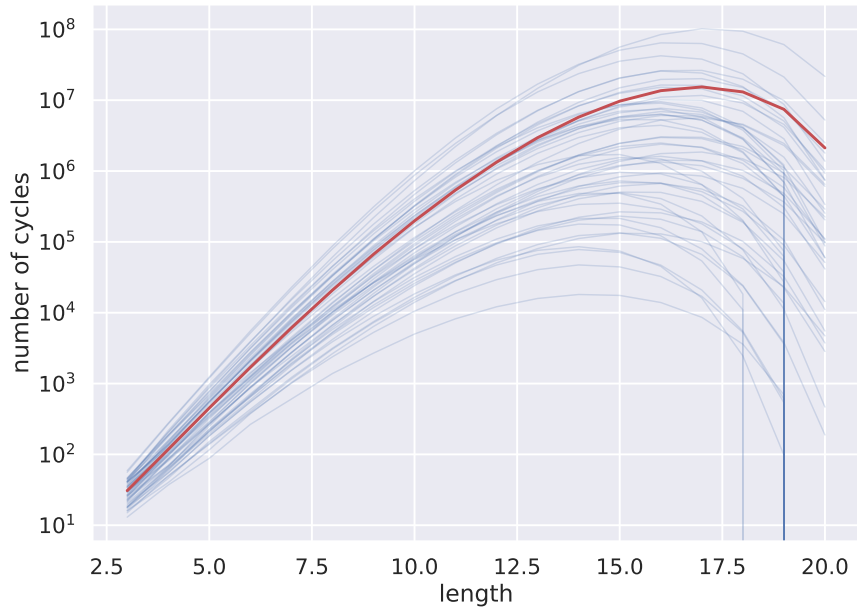
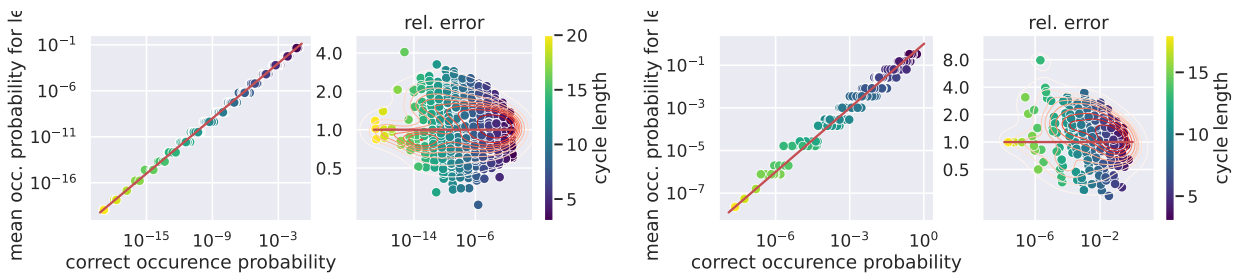


Figure 12: Number of simple cycles N_l on 50 graphs sampled from Erdős-Rényi with $n = 20, p = 0.3$. The red line indicates the a priori estimation \mathcal{N}_l . There is a large variance in the number of cells for a given l , especially as $l \rightarrow n$.

D.1 Approximation Accuracy



(a) Evaluation on the same cycles and graph sampled from ER with $n = 30, p = 0.5$ as Figure 7 (a).

(b) Evaluation on the same cycles and graph sampled from ER with $n = 30, p = 0.15$ as Figure 7 (b).

Figure 13: The approximation error of a hypothetical approximation that assigns each cycle the mean probability of all cycles with the same length, for a moderate configuration (a) and a sparse configuration (b). The estimation error is significantly larger than that of our approach, i.e., our approach detects significantly more than just the cycle length.

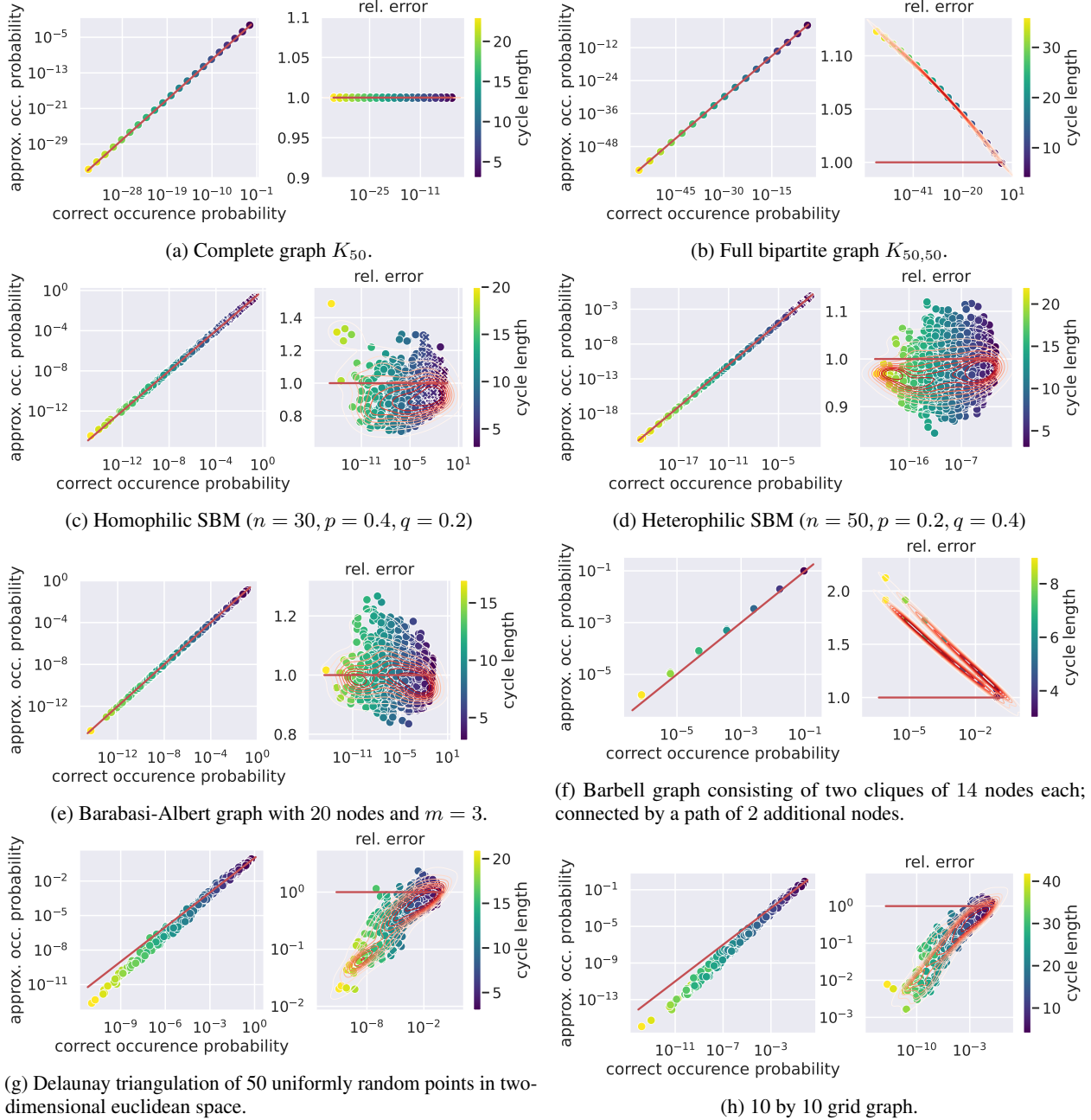


Figure 14: **The approximation error on different synthetic graphs.** Informally, we observe two graph properties that reduce accuracy. First, if the graph is not well-connected, the approximation over-estimates the occurrence probability. If the graph is planar (or rather, has a large diameter), it significantly underestimates. Both behaviors can be explained by the Laplacian random walk. In a globally disconnected network, the random walk stays closer to the target node than expected, and in the planar network it can go further away from it than expected. **a**: On the complete graph, our approximation is exact. **b**: On a full bipartite graph, there is a small systematic error. **c/d**: On both homophilic and heterophilic configurations of the Stochastic Block Model, our approximation is more accurate than expected, indicating that global connectivity, even with some biases, is sufficient. **f**: On the barbell graph, all cycles are contained in a smaller, complete subgraph. Since the model assumes a globally connected graph, the approximation fails in multiple points, e.g., assuming the target node is not always adjacent, the number of visited nodes that are adjacent, and assuming that the penultimate node has a higher likelihood of being chosen than other neighbors. The edge leading away from the fully connected subgraph results in a spurious difference of approximated occurrence probabilities. **g/h**: It is clear that the approximation results in a strong and systematic bias on tessellations of the plane, such as Delaunay triangulations or 2D grid graphs. Since the approximation assumes approximately even connectivity in multiple steps, the geometric structure differs greatly.

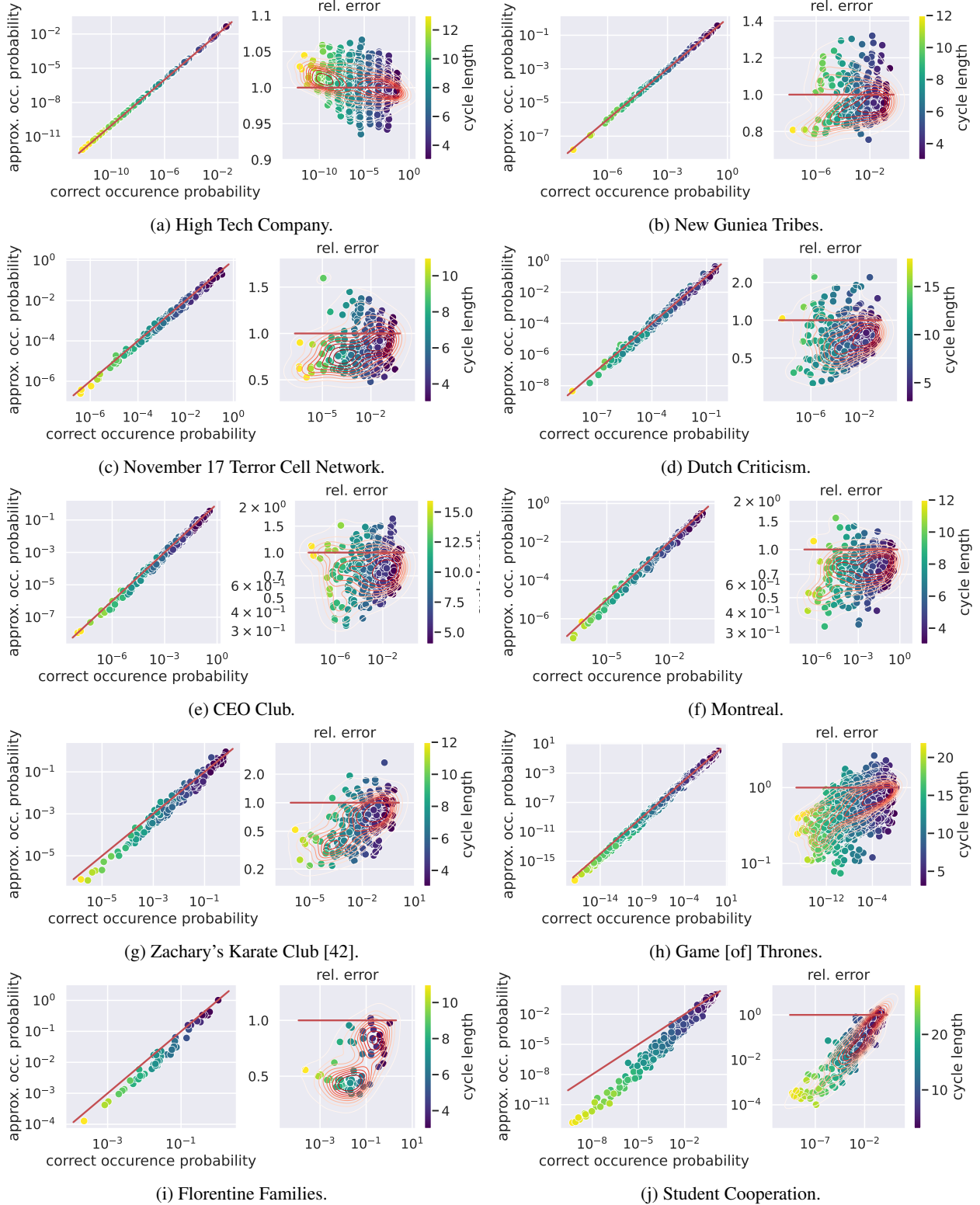


Figure 15: Accuracy of the approximated occurrence probability \tilde{p}_C on real-world datasets (unless otherwise noted retrieved from *Netzschleuder*, <https://networks.skewed.de>). On real-world data, we largely observe a small bias with a moderate variance in the approximation. For networks (g)–(i), there is a more systematic error. These three networks have a comparatively large diameter. A notable exception is j, which is globally nearly planar.

D.2 Count Estimation

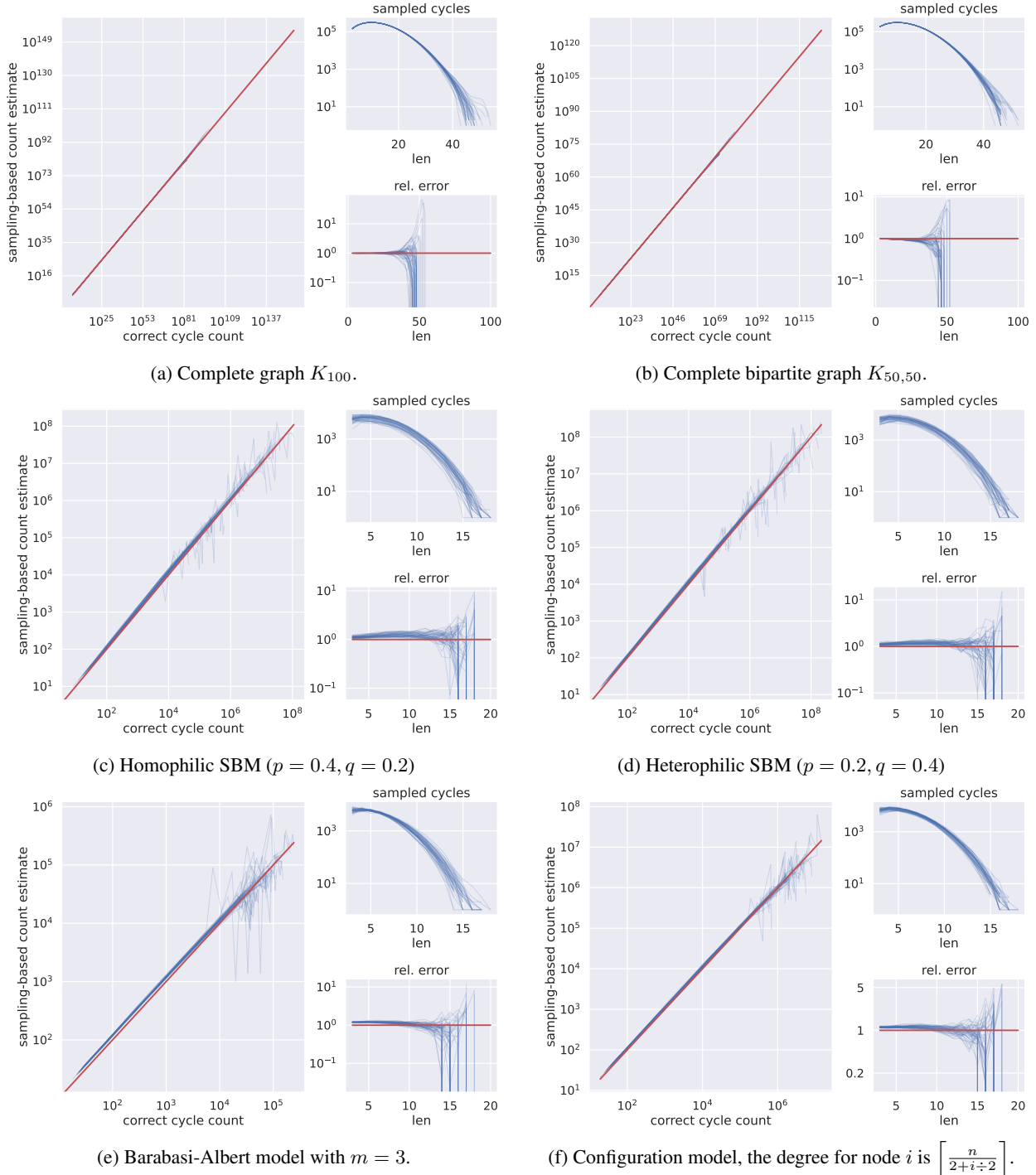


Figure 16: The estimated number of cycles for different lengths, number of sampled cells, and relative error by length on 50 graphs sampled from a homophilic (a) and heterophilic (b) SBM, each with two blocks of 10 nodes. In both cases, the accuracy is surprisingly good considering that the approximations assume an underlying ER-Graph. The accuracy is massively reduced for lengths where the sampled number of cells is too small.

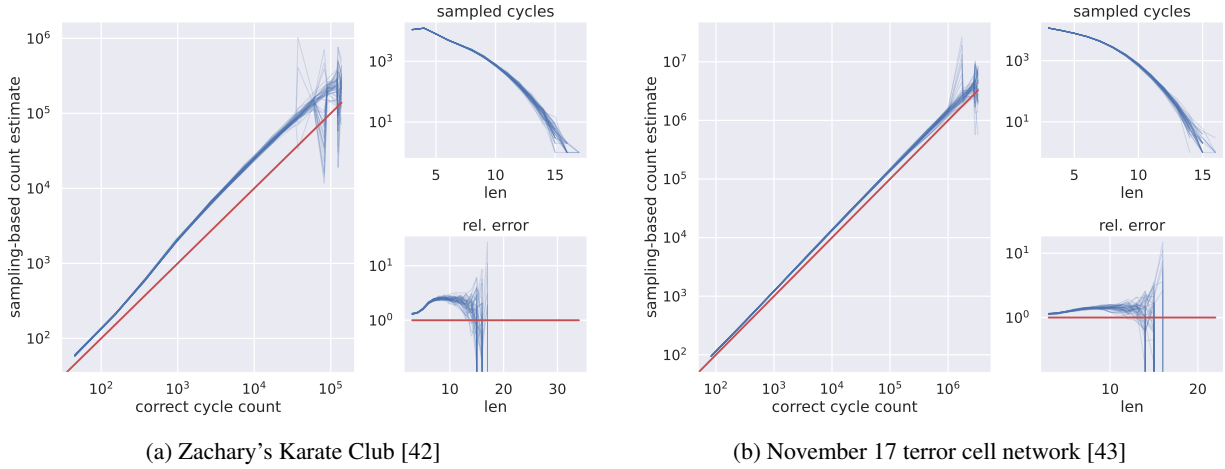


Figure 17: The estimated number of cycles for different lengths, number of sampled cycles, and relative error by length on 50 runs sampled on two real-world graphs. In both cases — given a reasonable number of occurring cycles — the estimation error is within an order of magnitude, but the karate club shows a significantly larger error. Given its very much non-ER-like structure, this is to be expected.

D.3 Properties of sampled complexes

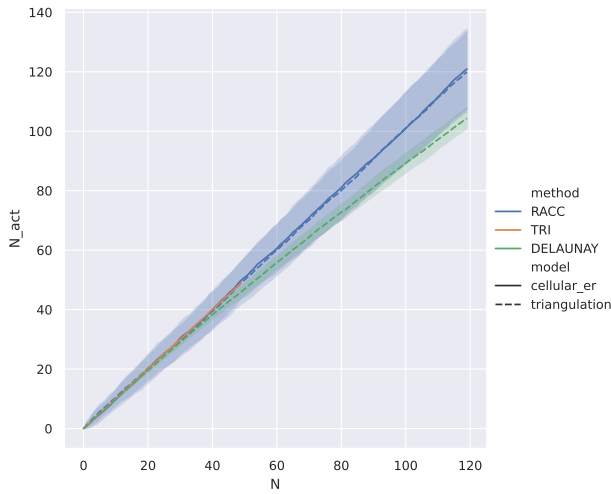
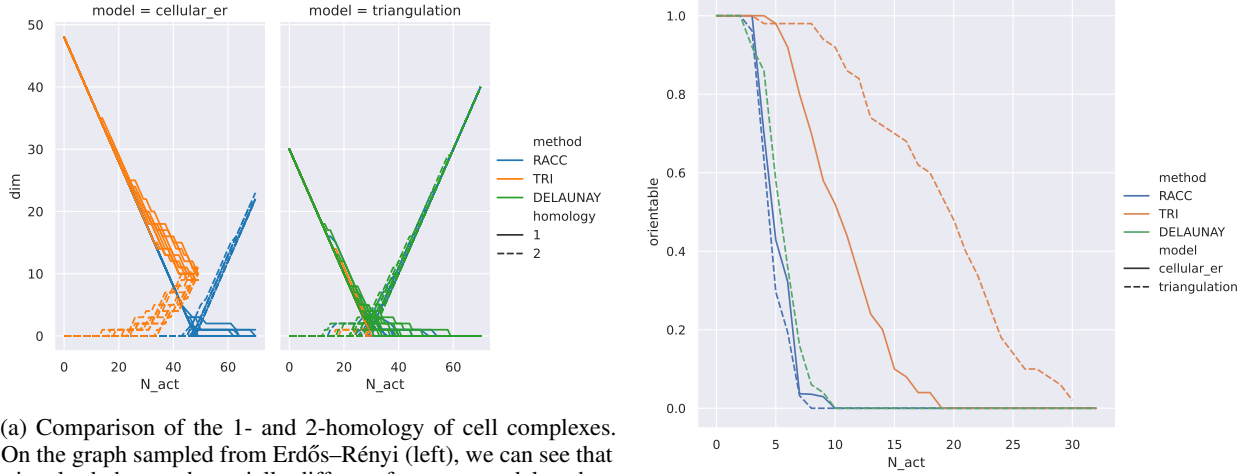


Figure 18: Comparison of the desired number of 2-cells to the actual number of cells, for our method (*RACC*), random triangles (*TRI*), and the ad-hoc triangulation-based model from [14] (*DELAUNAY*). Our method samples, in expectation, the correct number of cells, even on the graph of a delaunay triangulation, where the ad-hoc method slightly undersamples.



(a) Comparison of the 1- and 2-homology of cell complexes. On the graph sampled from Erdős–Rényi (left), we can see that triangles behave substantially different from our model as they start adding 2-cohomologies earlier and do not remove all 1-homologies. On the graph sampled from a Delaunay triangulation (right), triangles produce few 2-cohomologies; our model and the ad-hoc model behave similarly with regard to homologies.

(b) Comparison of the orientability of sampled complexes (fraction of samples that is orientable). On both graphs, TRI complexes are orientable with more added cells. On Delaunay, only few local structures admit non-orientability.

Figure 19: Analysis of random cell complexes, comparing our model (RCC) to the triangulation-based model from [14] (DELAUNAY) and randomly-selected triangles (TRI); 50 runs each. Evaluation uses both a graph sampled from ER ($n = 20, p = 0.3$) and a Delaunay triangulation ($n = 20$). (b) shows what fraction of sampled CCs is orientable, again showing a similar behavior for the two models, with triangles (SCs) deviating significantly.